Filtration, 1. Fundamentals

Siegfried Ripperger, Gonbach, Germany

Walter Gösele, Heidelberg, Germany

Christian Alt, München, Germany

ULLMANN'S ENCYCLOPEDIA OF INDUSTRIAL CHEMISTRY

Symbols

A:	cross-sectional area, filter area, m^2
α:	resistance of a porous medium
α_H:	cake resistance relative to cake thickness, m^{-2}
α_m:	cake resistance relative to dry mass, m/kg
B:	creep constant
β:	resistance of the filter medium, m^{-1}
C:	creep constant
c:	Concentration of the suspension
c_V:	solid concentration as a part of total volume
d_h:	hydraulic pore diameter of a porous structure
d_{pore}:	capillary diameter, m
d_S:	Sauter mean diameter of particles, m
E:	electrostatic potential at the solids surface, V
ε:	porosity of the porous medium
H:	cake thickness
I:	ionic strength, mol/L

DOI: 10.1002/14356007.b02_10.pub2

J: Boucher's filterability index, m^{-3}
K_H: proportionality volume of cake/volume of filtrate, m^3/m^3
K_m: proportionality mass of cake/volume of filtrate, kg/m^3
K_N: proportionality number of particles/volume of filtrate, m^{-3}
k: permeability of the filter cake $= 1/\alpha_H$, m^2
L: distance from the inlet face of the filter bed, m
λ: filter coefficient of deep bed filters, m^{-1}
m: mass of dry filter cake, kg
m_i: molar concentration of ion "i", mol/L
N: number of open pores
n: compressibility factor
η: viscosity, Ns/m^2
p_L: pressure in the liquid, Pa
p_S: compressive stress on the solids, Pa
Δp: pressure drop
p_c: capillary pressure, Pa
p_{ce}: capillary entry pressure, Pa
p_{ci}: capillary suction pressure, Pa
q: exponent describing blocking behavior
r: distance from the solids surface, m
r_D: Debye length, m
S_R: reduced saturation
S: saturation (volume of liquid/volume of pores)
S_v: specific inner surface
S_∞: irreducible saturation
t_{reg}: regeneration time for cleaning and preparing a run, s
Θ: dimensionless time
U_c: consolidation rate
V: volume of filtrate, m^3
$\dot{V}$: volumetric flow rate, m^3/h
V/A: specific flow rate or filtration velocity
z_i: valency of ion "i"
ζ: surface potential, V
Ψ: energy potential

Indices

av: average
e: end of filtration
H: related to cake thickness (height)
L: liquid
loc: local
m: related to cake mass
N: number
S: solid
w: wash liquor
pore: pore (volume)

1. Terminology

Filtration is the separation process of removing solid particles, microorganisms or droplets from a liquid or a gas by depositing them on a *filter medium* also called a *septum*, which is essentially permeable to only the fluid phase of the mixture being separated. The particles are deposited either at the outer surface of the filter medium and/or within its depth. The permeation of the fluid phase through the filter medium is connected to a pressure gradient.

This chapter deals only with filtration processes of solid–liquid mixtures (suspensions, slurries, sludges). For the treatment of gases by filtration see → Dust Separation.

Sometimes, however, purification of a liquid or gas is called filtration even when no semipermeable medium is involved (as in electrokinetic filtration).

The liquid more or less thoroughly separated from the solids is called the *filtrate, effluent, permeate* or, in case of water treatment, *clean water*. As in other separation processes, the separation of phases is never complete: Liquid adheres to the separated solids (*cake* with *residual moisture*) and the filtrate often contains some solids (*solids content in the filtrate* or *turbidity*).

The purpose of filtration may be clarification of the liquid or solids recovery or both. In *clarification* the liquid is typically a valuable product and the solids are of minor quantity and are often discarded without further treatment. If however, the solids are to be recovered, they very often have to be washed, deliquored and dried (see Fig. 1). In this article, *washing* means the cleaning of a product (filter cake) and it is distinguished from cleaning parts of the filter itself, which will be called *rinsing* (e.g., rinsing a filter screen or a filter cloth by jets of water). A further distinction is to be made between *washing* and *extraction* or *leaching*. *Washing* eliminates liquid contaminants from the pores between the

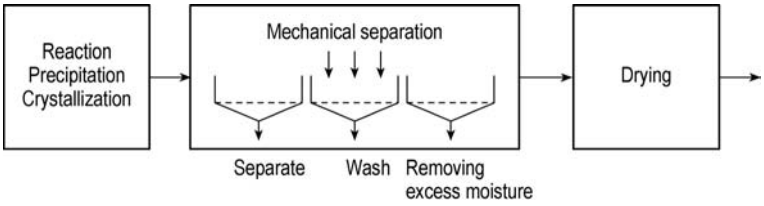

Figure 1. Solids processing chain

particles of a filter cake. *Extraction* recovers soluble matter out of the solid particles themselves (→ Liquid–Solid Extraction). The term *drying* means thermal drying, while the elimination of liquid from the filter cake by mechanical forces is called *deliquoring* or *dewatering*, e.g., deliquoring by a pressurized gas or by expression.

Filtration processes can be classified in accordance with different criteria:

1. *Location of particle retention*
   The particles can be separated on the outer surface of the filter medium (*surface filtration, cake filtration*) or inside of the filter medium (*depth filtration, deep bed filtration*)
2. *Generation of the pressure difference*
   Pressure filtration, vacuum filtration, gravity filtration, centrifugal filtration
3. *Operation mode*
   discontinuous, continuous, quasi-continuous. Dynamic filtration and static (normal) filtration. In case of dynamic filtration are during the filtration process mechanisms active which helps to reduce the build up of a filter cake. The most common dynamic filtration process is cross-flow-filtration
4. *Application*
   For example water filtration, beer filtration

Filtration is effected by application of a pressure difference which can be produced by a *pressurized fluid*, by a *vacuum*, by the *gravity* or by *centrifugal force* (see Fig. 2). *Pressure filtration* typically requires a pump for delivering the suspension to the filter. *Vacuum filtration* requires a vacuum pump. The pump evacuates the gas from a filtrate receiver, where the filtrate is separated from the gas. The filtrate is drained either by a barometric leg of at least 8 to 10 m or by a pump that is able to *run on snore* (i.e. with a deficiency of feed liquid so that it tends to draw in air). In some cases the liquid is allowed to flow through the filter medium only by gravity (*gravity filtration*). *Centrifugal filtration* is done in perforated centrifuge rotors (→ Centrifuges, Filtering).

In case of *vacuum filters* the cake is freely accessible. This facilitates automatic cake handling. However, vacuum filters cannot handle hot liquids, or solvents with high vapor pressure. The pressure difference across vacuum filters is very limited, and the residual moisture of the filter cake is higher than with pressure filters. *Pressure filters* allow high pressure differences. They are preferred when the product must be kept in a closed system for safety reasons, or if the residual moisture content is important. The handling of the filter cake is obviously more difficult in a pressure filter. Filtration by *centrifugal force* requires more technical equipment, but as a general rule it yields solids with lower residual moisture (→ Centrifuges, Filtering).

During a *dynamic filtration* the collected solids on the filter media are continuously removed, mostly with a tangential flow to the filter medium (*cross-flow filtration*). Cross-flow filtration is a standard operation with membranes as a filter medium. The flow parallel to the filter medium reduces the formation of a filter cake or

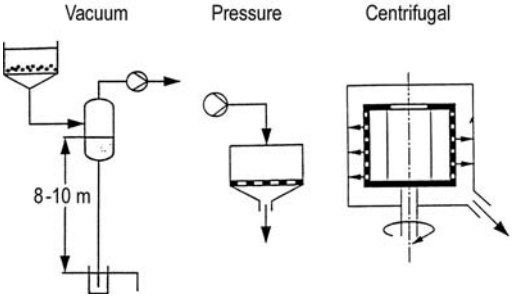

Figure 2. Driving forces in filtration

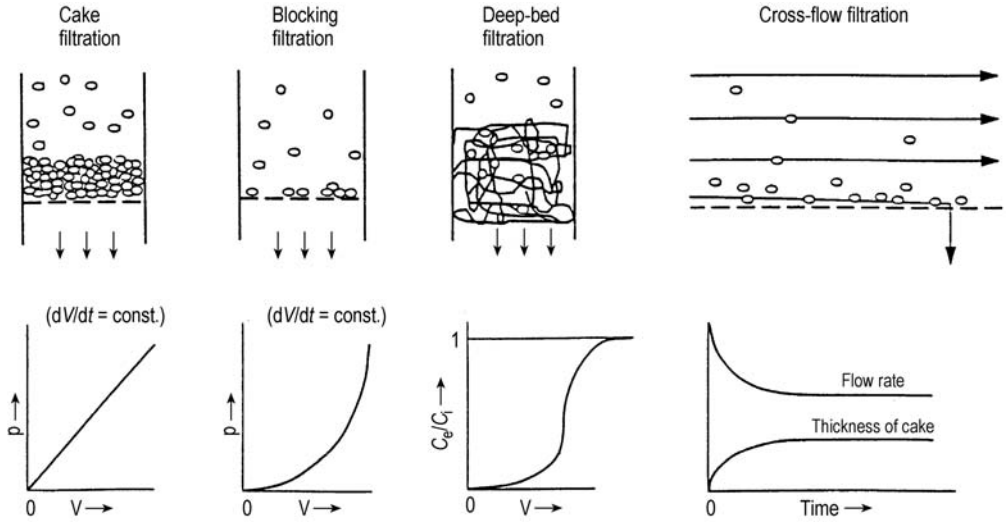

Figure 3. Filtration models

keeps it at a low level. So it is possible to get a quasi-stationary filtrate flow for a long time.

Various models have been developed to describe the physical process of filtration. This chapter concentrates on four idealized filtration models depicted in Figure 3.

Cake filtration is the most frequently used model. Here it is assumed that the solids are deposited on the upstream side of the filter medium as a homogeneous porous layer with a constant permeability. As soon as the first layer of cake is formed, the subsequent filtration takes place an the top of the cake and the medium provides only a supporting function. Thus, if the flow rate dV/dt is constant, the pressure drop will increase linearly, proportional to the quantity of solid deposited. This model can be applied especially for all hard, particulate solids.

Blocking Filtration. The pressure drop is caused by solid particles blocking pores. Soft, gelatinous particles retained by a sieve exhibit such a behavior. If the flow rate dV/dt is constant, the pressure drop increases exponentially with the quantity filtered, the number of open pores asymptotically approaching zero. The pores may belong to a filter medium (screen or filter layer) or it may be pores within a filter cake of coarse particles, which are blocked by migrating fine particles.

Deep Bed or Depth Filtration. Solid particles are retained in a deep filter layer. This takes place for example in sand filters for clarification of drinking water, which retain even colloidal particles. The typical effect of deep bed filtration is adhesion of solids to the grains of the filter layer. Only rather big particles are retained by the screening effect. When the filter bed has been saturated with solids, the solids concentration in the filtrate leaving the bed progressively approaches that of the incoming suspension.

Cross-Flow Filtration. In cross-flow filtration the suspension flows with high speed tangentially to the filter medium surface, preventing the formation of a filter cake. Only a small flow of liquid passes through the filter medium. A certain layer of solids accumulates in the boundary layer on the filter surface, and reduces the flow of filtrate. After an initial period, a dynamic equilibrium is established between convective transport of solids to the filter surface and removal of solids by hydrodynamic forces acting on the particles due to turbulence and diffusion.

Surface filtration is the antonym to depth filtration. The solids are retained on the surface of a filter medium. Generally the models of cake filtration or of blocking filtration can be applied.

Screening designates a classification process, which retains the particles below a certain size and lets pass the smaller ones through the

openings of the screen (→ Screening). Often the term *screening-filtration* is also used to designate a surface filtration with a screen as a filter medium. Its mode of action resembles screening (or straining) as long as the filter medium is clean, but it is clearly a cake filtration as soon as a layer of solids has formed.

2. Filtration Models

2.1. Calculation of the Pressure Drop over the Filter Medium and/or the Filter Cake

2.1.1. Definition of Filter Resistance and Cake Permeability: The Darcy Equation

The resistance to flow of a porous medium (filter medium or filter cake) can be described by Darcy's law [1] (see Fig. 4). Consider a liquid flowing through a filter cake (or a stream of water percolating through soil as considered by Darcy). The pressure drop Δp of this flow is proportional to:

1. The flow rate per unit area V/A (*specific flow rate* or *filtration velocity*)
2. The cake thickness H
3. The viscosity η of the liquid
4. A constant α_H describing the "specific filter resistance" of the cake:

$$\Delta p_1 = \left(\frac{\dot{V}}{A}\right) \cdot H \cdot \eta \cdot \alpha_H \qquad (1)$$

In SI units the unit of α_H must be m^{-2} in order to satisfy the Darcy equation (1). The reciprocal of the filter resistance α_H is also called permeability k of the filter cake:

$$k = \frac{1}{\alpha_H} [m^2]$$

Sometimes it is more convenient to define cake thickness in terms of solid mass m per unit filter area α_m (unit kg/m^2). This leads to a slightly different definition of filter cake resistance. A corresponding equation to the Darcy equation can be written with a constant α_m with the unit m/kg describing the resistance of the cake.

Then the following expression is obtained instead of Equation (1)

$$\Delta p_1 = \left(\frac{\dot{V}}{A}\right) \cdot \left(\frac{m}{A}\right) \cdot \eta \cdot \alpha_m \qquad (2)$$

For practical reasons the viscosity η is very often not measured separately. Then it is legitimate to include it in a term $\alpha_H\eta$ (unit mPa · s/m^2) or $\alpha_m\eta$ (unit mPa · s · m/kg), respectively.

Using this latter term $\alpha_H\eta$ or $\alpha_m\eta$ filter resistances lie between 10^{11} mPa · s/m^2 (filtering very rapidly) and 10^{16} mPa · s/m^2 (nearly unfilterable), or between 10^8 and 10^{13} mPa · s · m/kg, respectively.

2.1.2. The Equation of Kozeny and Carman

The resistance α of a porous medium depends on its size and number of pores and its porous structure. In a first approximation it can be related to hydraulic pore diameter of a porous structure d_h:

$$d_h = 4\frac{\varepsilon}{(1-\varepsilon)\cdot S_v}$$

ε is the *porosity (void volume fraction)* of the porous medium. S_v is the specific inner surface of the medium (filter medium or filter cake) related to the volume of solid mass. In case of a spherical particle system one can write:

$$S_v = \frac{6}{d_S}$$

d_S is the Sauter diameter, an average diameter of an particle size distribution, obtained by dividing the total volume of a particle by the total surface

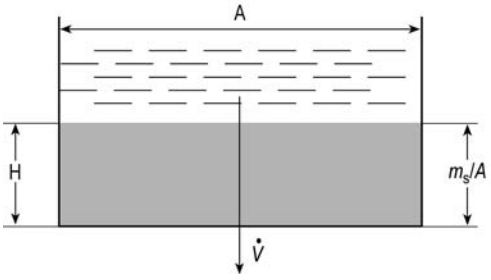

Figure 4. Definition of filter resistance
$\eta\alpha_H$ = Cake thickness H related filter resistance; $\eta\alpha_m$ = Solid mass related filter resistance

area. One can see that the specific surface and the hydraulic pore diameter depend strong on the particle sizes.

Based on a laminar flow inside a porous system with pores of a hydraulic diameter d_h one get in combination with the Darcy equation (1) an useful approximation for the specific resistance of a porous medium:

$$\alpha_H \approx 5 \cdot \frac{(1-\varepsilon)^2 \cdot 36}{\varepsilon^3 \cdot d_S^2} \approx 5 \cdot \frac{(1-\varepsilon)^2}{\varepsilon^3 \cdot S_v^2}. \quad (3)$$

The Equation (3) is known as the Kozeny–Carman equation. The theoretical basis of this equation is described in [2]. The filter resistance resulting from this equation is depicted in Figure 5 as a function of particle size d_S and porosity ε. In practical applications the filter resistances cover a very wide range of porosity. Fine particles, especially dry dust, often form cakes with surprisingly high porosities (see Fig. 6). The same quantity of powder (filter aid, mean particle size ≈ 5 µm) has settled in water with different pH and in air. The settling volume (and the clarity of the supernatant) is quite different. Filter resistance depends therefore to a large degree on particle sizes, cake porosity and hence in case of fine particles on the surface forces producing this porosity.

Filter media for surface and cake filtration are selected according to their pore diameter (≈ hydraulic diameter). To reduce their hydraulic resistance they are produced with a high porosity.

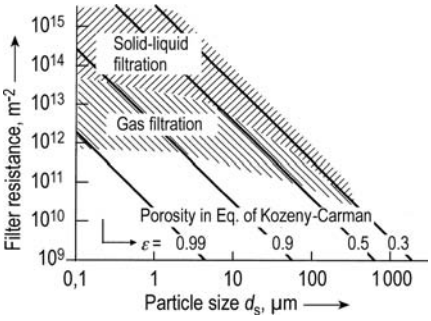

Figure 5. Filter resistance vs. particle size
The range of usual values is compared to the calculated lines according to Kozeny–Carman, Equation (3)

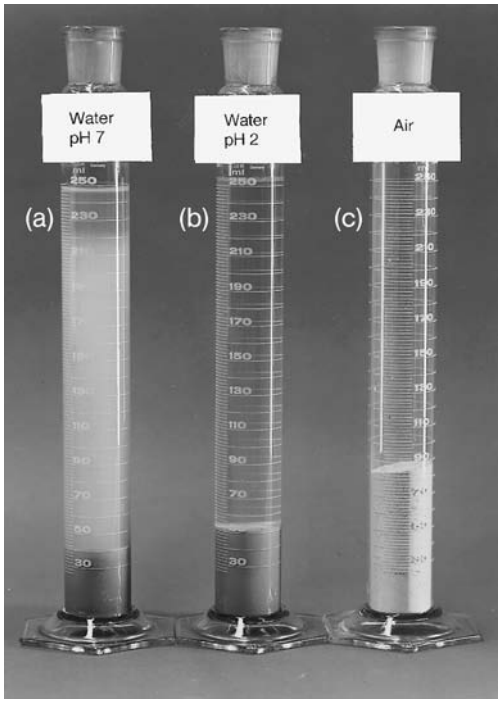

Figure 6. Settling volumina of the same quantity of filter aid (mean particle size ca. 5 µm) a) In water at pH 7; b) In water at pH 2; c) Dry powder compacted by its own gravity [5]

2.2. Cake Filtration

2.2.1. The "Cake Filter Equation"

The pressure drop in a filter is composed of a pressure drop Δp_1 across the cake according to Equation (1) and a pressure drop Δp_2 across the filter medium, which can be written as:

$$\Delta p_2 = \beta \cdot \eta \cdot \left(\frac{\dot{V}}{A}\right) \quad (4)$$

where β (unit m^{-1}) is the resistance of the filter medium.

The total pressure drop is therefore:

$$\Delta p = \Delta p_1 + \Delta p_2 = \alpha_H \eta \cdot H \cdot \frac{\dot{V}}{A} + \beta \eta \frac{\dot{V}}{A} \quad (5)$$

or

$$\Delta p = \Delta p_1 + \Delta p_2 = \alpha_m \eta \cdot \frac{m \cdot \dot{V}}{A^2} + \beta \eta \frac{\dot{V}}{A}$$

If the suspension is homogeneously mixed, the cake height H (or m/A) will be proportional to the quantity of filtrate. The influence of the concentration and cake porosity is described by the factor K_H:

$$K_H = \frac{c_v}{(1-\varepsilon)} = \frac{H \cdot A}{V} \tag{6}$$

or

$$K_m = \frac{m}{V} \tag{7}$$

where m represents the mass of particles in the filter cake, which is independet from the cake porosity.

With Equation (6) and (7) one obtain:

$$\Delta p = \frac{\alpha_H \eta K_H}{A^2} \cdot V \cdot \frac{dV}{dt} + \frac{\beta \eta}{A} + \frac{dV}{dt} \tag{8}$$

or

$$\Delta p = \frac{\alpha_m \eta K_m}{A^2} \cdot V \cdot \frac{dV}{dt} + \frac{\beta \eta}{A} + \frac{dV}{dt} \tag{9}$$

Equation (8) and (9) are identical under the generalization $\alpha_H \cdot K_H = \alpha_m \cdot K_m$. Nevertheless the distinction between both equations is useful for clarity.

The differential Equation (8) and (9) can be integrated either for constant flow rate or for constant pressure. Integration for constant flow rate $dV/dt = \text{const.}$ gives the trivial solution:

$$\Delta p = \frac{\eta \cdot \dot{V}}{A} \cdot \left(\frac{\alpha_H K_H}{A} \cdot V + \beta \right)$$

or

$$\Delta p = \frac{\eta \cdot \dot{V}}{A} \cdot \left(\frac{\alpha_m K_m}{A} \cdot V + \beta \right)$$

For $\Delta p = \text{const.}$ the integration yields:

$$dt = \frac{\alpha \eta K}{A^2 \cdot \Delta p} \cdot V \cdot dV + \frac{\beta \eta}{A \cdot \Delta p} \cdot dV$$

$$t = \frac{\alpha_H \eta K_H}{2A^2 \cdot \Delta p} \cdot V^2 + \frac{\beta \eta}{A \cdot \Delta p} \cdot V \tag{10}$$

or

$$t = \frac{\alpha_m \eta K_m}{2A^2 \cdot \Delta p} \cdot V^2 + \frac{\beta \eta}{A \cdot \Delta p} \cdot V \tag{11}$$

2.2.2. Evaluation of Experiments with Linear Diagrams

2.2.2.1. Linear Diagram in the Differential Form

It is often very helpful to plot the instantaneous resistance to flow as a function of the quantity filtered. The resistance is characterized by the pressure drop Δp related to the instantaneous flow rate dV/dt. Using Equation (4) or (5) this can be written as:

$$\begin{aligned} \frac{dt}{dV} &= \frac{\alpha_H \eta K_H}{\Delta p A^2} \cdot V + \frac{\beta \eta}{\Delta p A} \\ &= \frac{\alpha_m \eta K_m}{\Delta p A^2} \cdot V + \frac{\beta \eta}{\Delta p A} = b \cdot V + a \end{aligned} \tag{12}$$

As shown in Figure 7 A [6], interpolation gives a straight line with slope b and intercept a. The intercept

$$a = \frac{\beta \eta}{\Delta p}$$

represents the resistance at the very first moment of filtration, before a cake is formed, hence the resistance of the filter medium including the boundary layer to the cake.

The slope b contains the filter resistance α according to

$$b = \text{slope} = \frac{\Delta\left(\Delta p \cdot \frac{dt}{dV}\right)}{\Delta V} = \frac{\alpha \eta K}{A^2}$$

Inserting K_H or K_m (see Eqs. 6 and 7) respectively, leads to

$$\begin{aligned} \alpha_H \eta &= \frac{\Delta\left(\Delta p \cdot \frac{dt}{dV}\right)}{\Delta V} \cdot \frac{A^2}{K_H} = \frac{\Delta\left(\Delta p \cdot \frac{dt}{dV}\right)}{\Delta V} \cdot \frac{A \cdot V}{H} \\ &= \Delta\left(\Delta p \cdot \frac{dt}{dV}\right)_e \cdot \frac{A}{H_e} \end{aligned} \tag{13}$$

and

$$\begin{aligned} \alpha_m \eta &= \frac{\Delta\left(\Delta p \cdot \frac{dt}{dV}\right)}{\Delta V} \cdot \frac{A^2}{K_m} = \frac{\Delta\left(\Delta p \cdot \frac{dt}{dV}\right)}{\Delta V} \cdot \frac{A^2 \cdot V}{m} \\ &= \Delta\left(\Delta p \cdot \frac{dt}{dV}\right)_e \cdot \frac{A^2}{m_e} \end{aligned} \tag{14}$$

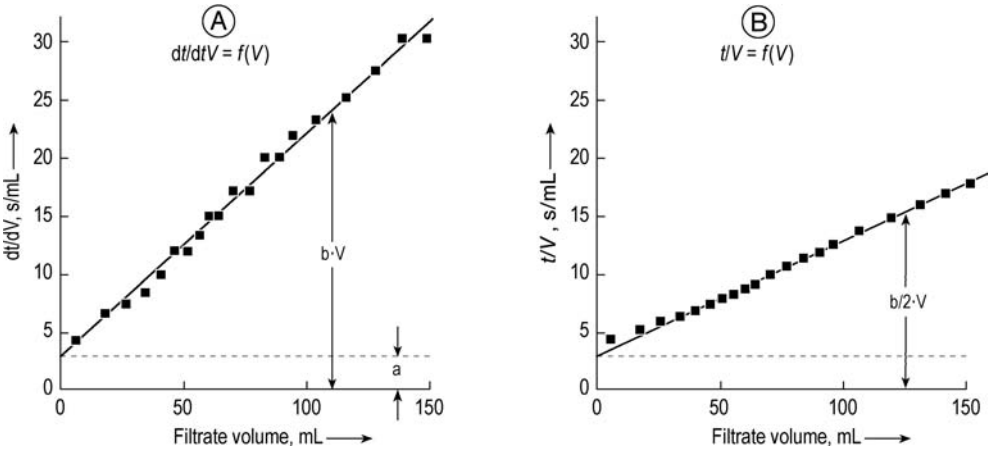

Figure 7. Linear plots according to Equation (12) and (15) [7] A) Linear diagram in the differential form; B) Linear diagram in the integrated form

2.2.2.2. Linear Diagram in Integrated Form

Another approach starts from the integrated filter Equations (10) or (11). The experimental results are plotted according to

$$\frac{t}{V} = f(V)$$

If the pressure is constant during the experiment, a straight line should be obtained

$$\frac{t}{V} = \frac{\alpha_m \eta K_m}{2A^2 \cdot \Delta p} \cdot V + \frac{\beta \eta}{A \cdot \Delta p} = \frac{\alpha_H \eta K_H}{2A^2 \cdot \Delta p} \cdot V + \frac{\beta \eta}{A \cdot \Delta p} = \frac{b}{2} \cdot V + a \quad (15)$$

This kind of plot is still very popular in practice because the evaluation is often easier than with Equation (12). Experimental values measured with a bucket and a stopwatch can be inserted directly into Equation (15), while for a differential diagram they have to be converted into momentary flow rates d*V*/d*t*.

On the other hand Equation (15) is correct only for Δp = const. Furthermore, the resulting diagram shows less clearly the deviations from linearity than a diagram based on instantaneous flow rates. If for example a cake stops growing and keeps a constant resistance this gives a well discernible plateau in a differential diagram, but only a gradual hyperbolic bend in the integrated diagram.

In case of a short filter cycle, the evaluation of the real beginning of filtration and the determination of the filter medium resistance could be problematic. Tichy [8] showed, that the crossing point of the combined graphs of Equation (12) and (15) gives a realistic starting point. He also showed, that the filter medium resistance based on filter experiments is much higher than the filter medium resistance evaluated on the pressure drop of a clean liquid (water). The reason for that the increase is an additional resistance based on a partial pore blocking of the filter medium during the first layer formation.

2.2.2.3. Example

The interpolation of the test results shown in Figure 7 leads to the intercept *a* and the slope *b*

$$a = 3.6\ \mathrm{s/mL} = 3.6 \times 10^6\ \mathrm{s/m^3}$$

and

$$b = \frac{28\ \mathrm{s/mL}}{150\ \mathrm{mL}} = 1.87 \cdot 10^{-11}\ \mathrm{s/m^6}$$

The following parameters are known or measured:

Filtration pressure	$= p = 1$ bar $= 10^5$ N/m^2
Filter area	$= A = 20$ cm$^2 = 20 \times 10^{-4}$ m^2
Viscosity	$= \eta = 0.001$ Pa · s $= 10^{-3}$ Ns/m^2

Cake height $= H_e = 37$ mm
Cake mass $= m_e = 24.3$ g
Volume of filtrate $= V_e = 154$ cm^3

Concentration factors:

$$K_H = \frac{A \cdot H_e}{V_e} = \frac{20 \cdot 10^{-4} \cdot 0.037}{154 \cdot 10^{-6}} = 0.481$$

or

$$K_m = \frac{m_e}{V_e} = \frac{24.3 \cdot 10^{-3}}{154 \cdot 10^{-6}} \cdot \frac{\text{kg}}{\text{m}^3} = 158 \frac{\text{kg}}{\text{m}^3}$$

The filter medium resistance can be calculated by

$$\beta = \alpha \cdot \frac{\Delta p \cdot A}{\eta} = 3.6 \cdot 10^6 \cdot \frac{10^5 \cdot 20 \cdot 10^{-4}}{10^3} \text{m}^{-1}$$
$$= 7.2 \cdot 10^{11} \text{m}^{-1}$$

If the porosity of the filter cake is $\varepsilon = 0.4$ and the part of liquid inside the filter cake is neglected, the solid concentration (as a part of total volume) in the suspension is:

$$c_v = \frac{A \cdot H_e \cdot (1-\varepsilon)}{V_e} = K_H (1-\varepsilon) = 0.289$$

From Equation (13) or (14) the cake filter resistance can be calculated by

$$\alpha_H = b \cdot \frac{A^2 \cdot \Delta p}{K_H \eta} = 0.187 \cdot 10^{11} \cdot \frac{400 \cdot 10^{-8} \cdot 10^5}{0.481 \cdot 10^{-3}} \text{m}^{-2}$$
$$= 1.56 \cdot 10^{14} \text{m}^{-2}$$

$$\alpha_m = b \cdot \frac{A^2 \cdot \Delta p}{K_m \eta} = 0.187 \cdot 10^{11} \cdot \frac{400 \cdot 10^{-8} \cdot 10^5}{158 \cdot 10^{-3}} \text{m}^{-2}$$
$$= 4.73 \cdot 10^{11} \frac{\text{m}}{\text{kg}}$$

2.2.2.4. Deviations from Linearity

Experimental data very often differ from the linear characteristic shown in Figure 7. The kind of deviation indicates the nature of secondary effects (see Fig. 8):

1. Theoretical linear curve without secondary effect (curve A, Fig. 8)
2. Some solids have settled before the filtration started, apparently increasing the resistance of the filter medium (curve B, Fig. 8)
3. The starting point of filtration was not measured correctly. The filtration started before the time measurement began (curve C, Fig. 8)
4. The solids settle out completely, increasing the speed of cake growth. At the end of filtration clear liquid flows through the cake of constant resistance (curve D, Fig. 8)
5. Only coarse particles settle. After some time only the remaining fines are filtered and the resistance increases progressively (curve E, Fig. 8)
6. Fine particles trickle through the cake and block the pores of the cake or of the filter medium. The process can perhaps be described as a blocking filtration (curve F, Fig. 8) (see Section 2.3). Further causes of deviations might be

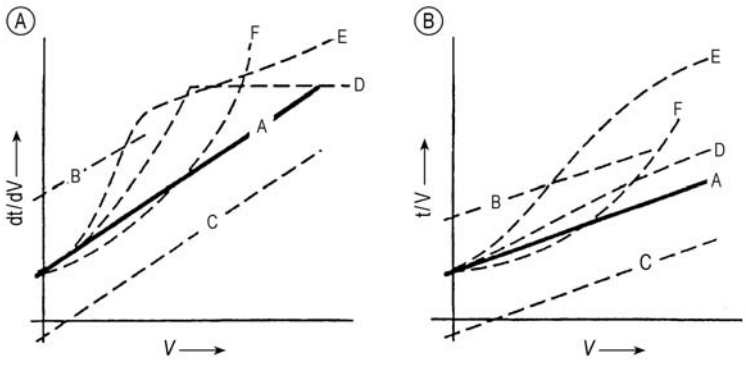

Figure 8. Typical deviations from linearity [7] A) Differential plot according to Equation (12); B) Integral plot according to Equation (15)

7. Determination of the beginning or the end point of filtration may not be correct. The end point is particularly difficult to determine if there is no sight glass in the filter. It is therefore common practice to neglect some points at the end of the measurement
8. Unusual properties of the suspension like foam bubbles or oil droplets, non-Newtonian rheology of the liquid and -isometric, platelike particles with special orientation can produce a great variety of effects
9. The solid may be so voluminous that it fills nearly the whole suspension. The process then resembles rather an expression than a filtration (Section 4.2).
10. Freshly precipitated solids sometimes continue to agglomerate or to "ripen" during filtration, changing their effective particle size and with it the filtration properties.

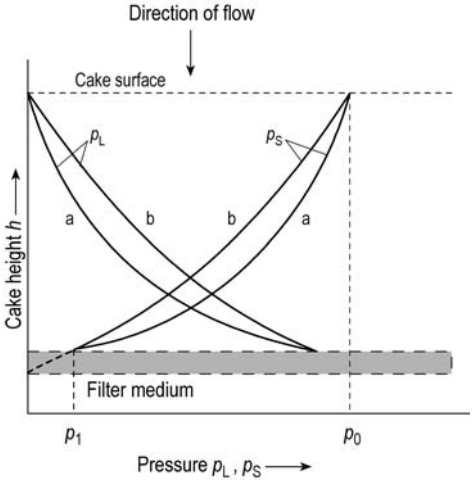

Figure 9. Hydraulic pressure p_L and solids pressure p_S as function of cake height
Curve a represents a more compressible cake than curve b

2.2.3. Compressible Cake Filtration

Most filter cakes are compressible, which means that their porosity decreases and their resistance increases with growing pressure. An *x*-fold increase in filtration pressure therefore normally gives rise to a less than *x*-fold increase in flow rate. The compression of the cake is caused by the compressive stress p_s on the particles and their framework which is caused by the drag forces of the flowing liquid (see Fig. 9). The loss in liquid pressure dp_L over a short distance dh translates into an increase of solids pressure dp_S, the sum of both pressures at a certain height in the cake h keeps constant:

$$dp_S = -dp_L$$

$$p_S + p_L = p_0$$

The *local filter resistance* α_{loc} in the cake is a function of the local compressive stress p_S and it is therefore low at the surface of the cake and high near the interface with the filter medium. The relationship between the resistance and the compressive stress $\alpha_{loc} = f(p_S)$ can be measured with a compression permeability cell (CP cell) (→ Filtration, 2. Equipment, Chap. 2.)

Only the *average resistance* α_{av} of a filter cake (all layers combined) is important for practical scale-up purposes. It can be calculated from $\alpha_{loc} = f(p_S)$ measured with a CP-cell [9]

$$\alpha_{av} = \frac{\Delta p}{\int_0^p \frac{dp}{\alpha_{loc}}}$$

Normally however, it is much easier to measure α_{av} directly with filtration experiments in a pressure filter as described in → Filtration, 2. Equipment, Chap. 2.. The uneven distribution of local porosity and filter resistance is then included in the measured value. In this case the pressure difference during the experiment must be the same as in the factory equipment.

The dependence of filter resistance α_{av} or α_{loc} on pressure can be approximated with different equations. Over a limited pressure range Equation (16) can be used

$$\alpha = \alpha_0 \cdot \left(\frac{p_S}{p_o}\right)^n \tag{16}$$

α_0 is the resistance at a standard pressure drop p_0 and n is a compressibility index (equal to zero for incompressible cakes). The parameters can be determined easily from a logarithmic plot $\alpha = f(p_S)$, where the slope indicates the compressibility factor n. Introducing α_{loc} according to this approximation into Equation (13) or (14), it can be shown that for $0 < n < 1$

$$n_{av} = n_{loc} \tag{17}$$

$$\alpha_{0,av} = (1-n)\cdot\alpha_{0,loc} \quad (18)$$

Thus the approximation Equation (16) has the advantage that it applies to both the local and the average resistance. However, such an approximation is valid only for a limited range of pressures and Equation (17) and (18) are restricted to $0 < n < 1$.

TILLER and coworkers [10] give an integration of the filter equation also for $n > 1$. According to their equations the flow rate quickly reaches a constant value with increasing pressure. For practical purposes it can be approximated that such "supercompactible" filter cakes with $n > 1$ (e.g., a great number of waste water sludges) yield the same flow rate independently of the pressure applied: increasing pressure only increases the compressed layer adjacent to the filter cloth. (The hypothetical cake which yields the highest flow at an "optimal pressure" and less flow at higher pressures apparently does not exist. In practical application, however, the output of a filtration may be best with moderate pressure, since this avoids excessive blocking of the filter medium).

For practical purposes Equations [16–18] are often ignored and compressible cakes are treated with the same equations as incompressible cakes, provided α is defined as average specific cake resistance under the conditions of operation.

Concerning deliquoring of compressible cakes, it is important to know that the porosity is unevenly distributed after filtration. The filter resistance often is concentrated in a thin, compressed layer facing the filter medium, the rest of the cake being very porous and wet. Deliquoring by expression (see Section 4.2) will then be very effective, even at moderate pressures, since it acts also on the upper layer of the cake.

2.3. Blocking Filtration and other Modes of Filtration

2.3.1. Complete Blocking Filtration

According to the idealized idea of complete blocking filtration, every particle in the suspension is retained on the filter medium and blocks (seals) one pore. The remaining number of open pores is then given by

$$N(t) = N_0(1-K_N\cdot V_L)$$

where N_0 is the number of pores in the clean filter medium, $N(t)$ is the remaining number of open pores, and K_N (m^{-3}) is the concentration of particles by number in the suspension. At constant pressure drop the volume of filtrate $V(t)_{\Delta p}$ = const. can be descibed by [11]

$$V(t) = \frac{1}{K_N}\cdot[1-\exp(-K_N\cdot\dot{V}_0\cdot t)]$$

with $\dot{V}_0(m^3/s)$ being the flow rate at the start of filtration with a clean filter medium.

2.3.2. Intermediate and Standard Blocking Filtration

In real filtration processes not every particle in the suspension will block a pore of the filter medium. Some particles will be retained by adhesion to the walls of a pore without blocking it totally; others will pass through the filter medium without being retained at all. Different formulae (or *filtration laws*) exist to describe such moderate blocking. A generalized model is based on Equation (19) and (20)

$$\frac{d^2t}{dV^2} = \text{const}\cdot\left(\frac{dt}{dV}\right)^q \quad (19)$$

for constant pressure filtration and

$$\frac{d(\Delta p)}{dV} = \text{const}\cdot(\Delta p)^q \quad (20)$$

for constant rate filtration.

The exponent q in this equation varies between 0 and 2 and describes the *blocking speed*:

$q = 0$ cake filtration, slow blocking
$q = 1$ so-called intermediate filtration
$q = 3/2$ so-called standard blocking filtration
$q = 2$ complete blocking.

A summary of the corresponding equations for flow rates and filtrate quantities is given in [12, 13]. Figure 10 visualizes some examples: Surface straining represents the classical example of complete blocking ($q = 2$), but also depth straining follows the same characteristic. Normal depth filtration in contrast (with particles much smaller than the filter pores) leads to pressure drop by diminishing pore size and can be described by the standard blocking equation ($q = 3/2$).

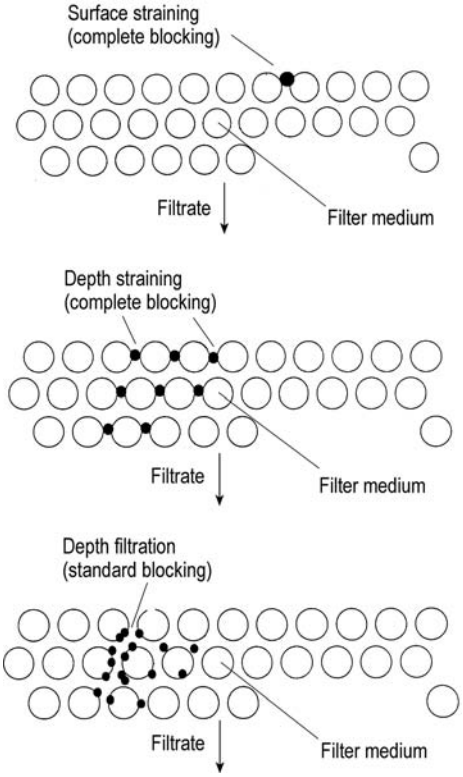

Figure 10. Three possible modes of filtration: Surface straining and depth straining are described as *complete blocking* ($q = 2$); depth filtration of particles much smaller than the pore size is best described as *standard blocking* ($q = 3/2$) [12]

In most filtrations it is highly probable that more than one filtration mode occurs. Cake filtration for example often is preceded by an initial period before cake build-up which can be described as standard blocking. This period is characterized by depth filtration (particles penetrating into the filter medium) and/or by fines passing through the filter medium (creating initial turbidity of the filtrate). For scientific investigations it may then be helpful to identify the filtration mechanism more precisely by parameter-fitting the experimental data and quantifying the above-mentioned "blocking speed".

2.3.3. Simplified Evaluation of Experimental Data

A very pragmatic approach is often used to describe the mode of filtration. The pressure drop at constant flow rate is depicted on a semi-logarithmic scale as a function of the volume filtered. Normally the values can be approximated by a straight line according to [14]

$$\log\left(\frac{p}{p_0}\right) = -J \cdot V_L \tag{21}$$

For the flow rate at constant pressure drop the same approximation holds

$$\log\left(\frac{\dot{V}}{\dot{V}_0}\right) = -J \cdot V_L \tag{22}$$

Here p_0 is the initial pressure drop of the clean filter; and the gradient J, which represents something like the above-mentioned blocking speed, is *Boucher's filterability index*. If $J = 1$ Equation (21) and (22) are identical to an *intermediate filtration* with $q = J = 1$. However, for other values of J the physical meaning of J is unclear. For scientific purposes this approach is therefore not so well accepted. For practical purposes, however, it is very useful.

2.4. Depth Filtration

2.4.1. Depth Filtration Mechanisms

In depth filtration (as opposed to surface filtration), the solid particles are separated mainly by deposition within the pores of the filter medium. The filter medium may consist of

1. A 0.5 to 3 m bed of coarse grains (e.g., deep bed of sand 0.3 – 5 mm)
2. A layer of a few centimeters of fibers (e.g., wound or resin bonded cartridge filters)
3. Sheets of a few mm thickness (e.g., sheet filter medium made of cellulose)
4. A layer of granular filter aid (e.g., precoat layer)

All these filter media have pores that are larger than the particles to be retained. The particles stick in the pores by adhesion or sterical stabilization and their accumulation increases the pressure drop, so that the filter must be cleaned or replaced periodically. This is why depth filtration should be used not to recover solids from a suspension such as cake filtration, but instead to produce a very clean effluent from suspensions

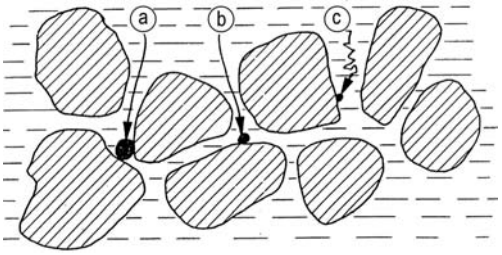

Figure 11. Retention mechanisms in a deep bed filter a) Particles > 10 μm are retained by mechanical interception; b) Particles of ca. 1 μm size are subject to inertial impact and adhesion; c) Particles <1 μm follow mainly Brownian diffusion and adhesion

with very low solids loading (typically < 0.1 g/L) and with very fine particles. Depending on the particle size, the prevailing effects of retention are summarized in Figure 11:

1. Particles larger than the pores are trapped mechanically. This is typically true for particles $\gg$ 10 μm
2. Particles 1 – 10 μm in diameter hit the solid surface mainly due to inertia effects and stick there due to a sterical stabilization and surface forces
3. Particles < 0.1 μm reach the solid surface mainly because of diffusion and stick there due to surface forces

In the range between 0.1 and 1 μm the transport mechanisms to the inner surface of both inertia and diffusion are small and hence a minimum in the effectiveness of depth filters is observed.

Thus the transport of particles to the solid surface is rather well explained and can be described mathematically. However, the mechanism of adhesion to the filter grains and the resulting *sticking probability* is not well-understood. Consequently the clarification effect must be summarized in an empirical *filter coefficient* λ describing the local decrease in concentration of the suspension flowing through the bed:

$$-\frac{\partial c}{\partial L} = \lambda \cdot c$$

where c is the concentration of the suspension and L is the distance from the inlet face of the filter. For uniform conditions, this differential equation can be integrated:

$$c = c_0 \cdot \exp(-\lambda_0 \cdot L)$$

here λ_0 is the initial filter coefficient of a clean filter medium. As soon as the medium is loaded with solids, its efficiency will change and that is why the solution of the differential equation becomes rather difficult. Different models exist to describe the process, but they are rarely used for practical purposes. To find a suitable filter medium in a depth filter which shows good retention efficiency over a long cycle time, laboratory tests over a realistic cycle time have to be carried out with filter layers of realistic depth.

The *pressure drop* in a depth filter can be interpreted as an effect of two different phenomena of blocking filtration:

1. The filter media exhibit a resistance to flow, which is increased by the solids deposit in the pores. The quantity of deposit is generally small compared to the pore volume, and the additional pressure loss per unit depth can be described as proportional to the local specific deposit. For constant solids concentration at the inlet and constant retention the increase in this pressure drop with time is therefore approximately constant.
2. In addition there is often a pressure drop due to deposits on the surface of the filter bed. This is a typical blocking filtration and can be described by Boucher's law (Eqs. 21 and 22).

The total pressure drop of a depth filter at constant flow rate can then be approximated by an equation of the type

$$p(t) = \text{const}_1 \cdot t + \text{const}_2 \cdot e^{J \cdot t}$$

The pressure drop should be measured in a test filter with a vertical height close to that of the full-scale unit (Fig. 12 A) [15]. For the case that the driving force is gravity, the pressure profile is shown in Figure 12 B. In the static equilibrium, at flow zero, 1 m of pressure head is gained for every meter of depth. The downstream consumers may then draw a constant flow rate. When flow has started, the pressure drop within the medium increases linearly with depth. As solids are deposited in the pores, the local pressure loss will increase in the upper layers and the pressure line becomes distorted. When the pressure line touches the atmospheric pressure value, the

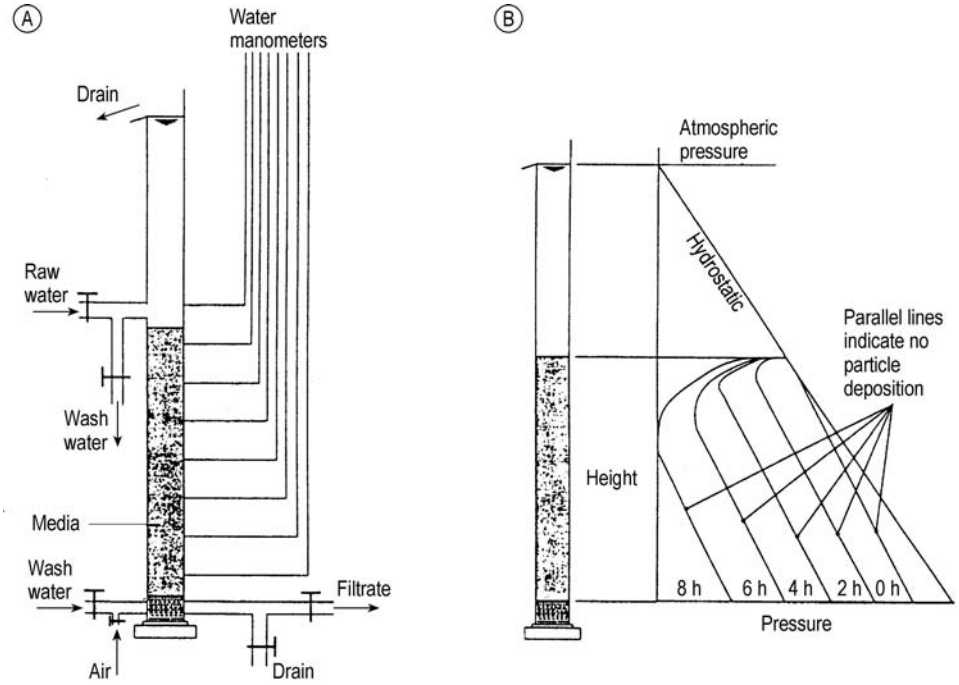

Figure 12. Laboratory test equipment for sand filters A) Test filter; B) Pressure profiles in test filter [15]

required flow cannot be maintained and the filter should be cleaned.

2.4.2. Cleaning and Sizing of Deep Bed Filters

Depth filters in form of deep bed filters (e.g., sand filters) [16, 17] can be cleaned by back-flushing. The flow is reversed to wash off deposited solids and flush them, e.g., to a wastewater station. Often air scour is used to increase the movement of the particles and reduce the amount of water necessary for fluidization. A typical set of data of a sand filter for cleaning of water could be [18]:

Medium depth	1 m
Medium size	0.5–1 mm (as uniform as possible)
Flow rate during filtration	5–10 $m^3\ m^{-2}\ h^{-1}$
Flow rate air scour	60 $m^3\ m^{-2}\ h^{-1}$ for 10 min
Flow rate water backflow	15–30 $m^3\ m^{-2}\ h^{-1}$ for 3–8 min after air scour

During backflow the sand grains are classified, the smallest ones are entrained to the top, the coarse ones sink to the bottom of the filter bed. This effect is undesired, since it leads to premature blocking of the top layer. Therefore it is important to use sand with grain sizes as uniform as possible.

The sizing of a deep bed filter consists of the following steps:

1. Preselection of the filter material by comparative laboratory tests with small layers of different materials under standard conditions and with the filtrate quality as a criterion
2. Selection of the right grain size in pilot tests with a filter column of 1 m height and a realistic flow rate and pressure drop

The minimum diameter of the cylindrical bed is 150 mm. If necessary the grain size must be adapted so that the bed is saturated (the filtrate gets turbid) at the same time as the maximum pressure drop is reached. If the maximum pressure drop is reached first, the grains should be coarser and vice versa. The ability to clean the filter bed by back-flushing should also be tested.

As mentioned above the sand grains are classified during back-flush and the uppermost layer is most efficient in collecting and becomes

clogged rapidly by captured solids. This disadvantage is diminished when a second layer of coarse material with lower specific weight is added on top of the sand layer. During backflow these low density grains collect at the bed surface and form a coarse layer able to retain a great quantity of dirt (so-called *multimedia filters* or *dual media filters*, e.g., with a layer of anthracite particles 1–2 mm in size on top of a main layer of sand grains 0.5–1 mm in size.)

Other designs of sand filters convert the disadvantage of classification into an advantage by operating in the upflow mode with filtering and back-flushing from below. This offers the advantage that large quantities of incoming dirt are retained in the lower layer of sand, which contains the coarser grains and larger pores. These upflow filters however need special safeguards against breakthrough of dirt when the pressure drop becomes high.

In order to increase the retention capacity in a given volume, it has also been proposed to use porous grains instead of sand grains. Small pieces of polymeric foam have indeed this effect [19]. Cleaning by simple back-flush is, however, not possible with this material, it must be cleaned by back-flush combined with compression. Therefore this method has not yet found practical application.

Quasi-continuous operation can be achieved using two ore more conventional deep bed filters in parallel. Truly continuous deep bed filters operates in the normal manner expect a portion of the filter bed is continuous or intermittently removed from the lower layer, cleaned to removed the contaminant and then automatically returned to the top of the filter bed. The cleaning and transport of the particles is mostly realized in the same time form of a hydraulic transport from the bottom to the top of the filter bed.

2.5. Cross-Flow Filtration

Cross-flow filtration is a form of a dynamic filtration. In cross-flow filtration the build-up of a filter cake on the surface of the filter media is hindered by a strong flow tangentially (parallel) to the filter surface. Clear liquid passes through the filter medium (mostly a membrane) and the concentrate (respectively the retentate) with higher concentrations of the rejected components is discharged from the filter. The cross-flow stream over the filter media has often a linear velocity in the range of 1 to 6 m/s. This cross-flow is achieved in most cases by pumping the suspension through a membrane module, which e.g., contains the membrane in form of a bundle of membrane tubes (→ Filtration, 2. Equipment, Section 10.1.). Alternatively the cross-flow is achieved by rotating inserts. The limitation of the deposition of particles and macromolecules on the membrane surface enables to filter very fine particles, which otherwise would form a cake with prohibitively high resistance. Even submicron, nonparticulate matter can be retained by membranes with a corresponding separation characteristic according to this principle. The shearing action on at the membrane surfaces limits the deposition of retained matter due to lift forces and diffusion processes back from the membrane. In normal operation the filtrate (respectively permeate) is collected and the concentrate is re-circulated until the desired concentration of retained components is achieved, or pumping can not be longer performed due to raised viscosity of the suspension. Typical units comprise one ore more membrane modules and a recirculation pump.

In this chapter a short overview will only be given, covering both the filtration of particles and the separation of nonparticulate matter. For more details see → Membranes and Membrane Separation Processes, 1. Principles. Depending on the size of the species retained, a distinction is made between microfiltration, ultrafiltration, nanofiltration, and reverse osmosis. Typical parameters of cross-flow filtration are summarized in Table 1.

Cross-flow Microfiltration. Microfiltration retains particles and microorganisms down to 0.1 μm in size. In steady-state cross-flow filtration these particles are conveyed onto the membrane by convection due to the filtrate flow and transported away from it by hydrodynamic lift forces due to the parallel shear flow (forces F_Y and F_L in Fig. 13). For particles below a certain size the lift force becomes smaller than the convection, $F_L < F_Y$, and they are deposited on the membrane [20]. After deposition they are retained by van der Waals' adhesion forces F_A and not easily swept away even if there is no filtrate flow (irreversible cake formation). In case

Table 1. Typical parameters of cross-flow filtrations

	Microfiltration	Ultrafiltration	Nanofiltration	Reverse osmosis
Cut-off size	> 100 nm	10–100 nm 10^3–10^5 g/mol	> 1 nm 200–10^3 g/mol	< 10^3 g/mol
Transmembrane pressure	0.02–0.5 MPa	0.2–1 MPa	0.5–3 MPa	2–20 MPa
Permeate flow	50–1000 L m^{-2} h^{-1}	< 100 L m^{-2} h^{-1}	< 100 L m^{-2} h^{-1}	10–35 L m^{-2} h^{-1}
Cross-flow speed	2–6 m/s	1–6 m/s	1–2 m/s	< 2 m/s
Important mechanism of retention	screening by the pores of the membrane	screening by the membrane and the gel layer	electrostatic repulsion and screening	solubility and diffusion in the membrane
Important mechanism of transport	hydrodynamic lift force	back-diffusion	back-diffusion	back-diffusion

of a steady-state microfiltration there is an equilibrium between the lift force and the drag force due the convection by the filtrate flow and a critical particle size. This steady-state flow is often mentioned as critical flux. In most practical applications also colloidal particles are present and they are transported according to the mechanisms of ultrafiltration or they are able to permeate through the microporous membrane of microfiltration. The cut-off size of a microfiltration membrane is usually defined as the size of particles of a test suspension (generally a suspension of microorganisms) which are nearly absolute retained.

Ultrafiltration retains colloidal particles or macromolecules. The cut-off sizes are ca. < 0.1 µm. Such particles are subject to Brownian diffusion (Br in Fig. 13) and only weakly influenced by the hydrodynamic lift force [21]. The smaller these particles are, the more they are transported away from the filter medium by diffusion. This is why in ultrafiltration the smaller particles are preferably swept away and the bigger ones are collected on the membrane (contrary to microfiltration). The cut-off size of an ultrafiltration membrane is usually defined as the molar mass (in g/mol) of a test solution (generally protein or dextran molecules of defined molar mass in the range of 10^3–10^5 g/mol). In practical application the cut-off size depends not only on the pore size of the membrane, but to a large degree on a *gel layer* on the membrane consisting of retained colloids.

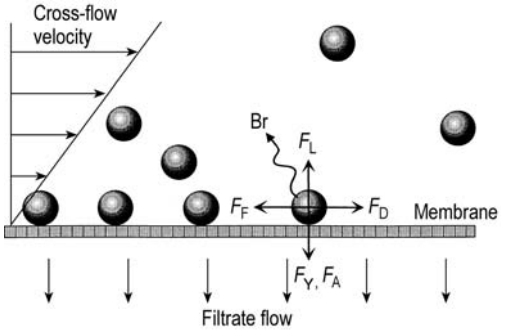

Figure 13. Forces and transport effects onto a particle in cross-flow filtration
Br = Brownian motion; F_A = adhesion to the membrane; F_D = drag from the cross-flow; F_F = friction force; F_L = hydrodynamic lift force; F_Y = drag from the filtrate flow

Nanofiltration combines features of ultrafiltration and reverse osmosis with a high selectivity. Its name is derived from its approximate cut-off size of some nanometers or more exactly molar masses of 200–600 g/mol. This is achieved with special nanofiltration membranes which still have pores of a defined size, but their retention depends also on the electrostatic charge of the molecules to be separated (bivalent anions are typically retained).

Reverse osmosis retains molecules or ions using selective membranes without pores. Certain molecules permeate through the membrane because they are soluble in the membrane material. Other molecules are not (or less) soluble and are retained (or concentrated) on the upstream side of the membrane. A particular feature of reverse osmosis is the high pressure required to overcome the osmotic pressure of the retained molecules. An important application is desalination of seawater. In the food industry it is applied to concentrate juices and other sugar solutions at low temperatures.

3. Washing of Filter Cakes

3.1. Basic Effects, Mass Balances

Cake filtration is often combined with washing and deliquoring (respeclively dewatering) of the filter cake. The purpose of washing is to remove the mother liquor left behind in the cake after filtration when this liquid is regarded as contaminant or must be recovered as a valuable component. Wash liquid flows through the filter cake and displaces the mother liquor, a mixture of both liquids leaving the cake as a wash filtrate. The concentration in this filtrate may help to explain some basic facts. In Figure 14 this concentration is reported as a function of the filtrate volume V. In the beginning it is $c_0 = 1$ (concentration of contaminant in the mother liquor). Four characteristic curves are reported:

Curve a represents the idealized piston flow. The pore volume V_{pore} is ideally displaced and leaves the cake with the concentration $c_0 = 1$. In this idealized case the washing would be finished with a quantity of wash liquid V_w equal the pore volume or the *washratio* can be expressed as:

$$\frac{V_w}{V_{pore}} = 1$$

Curve b takes into account that even in an idealized cake the flow passes through streamlines with different lengths and speeds. Because of this "axial dispersion" the required wash volume is several times the pore volume. The *washratio* can be expressed as:

$$\frac{V_w}{V_{pore}} > 1$$

Curve c is still more realistic; taking into account that a filter cake contains stagnant zones or dead-end pores, which are not reached by the flow. They deliver their contaminant content by diffusion to the effluent. Diffusion is an asymptotic process and depends on the time elapsed, not on the quantity of liquid. This curve is typical for most washing processes. The first part depends on the *washratio*, the end, however, is an asymptotic process depending on time.

When the curves a, b and c were drawn, it was supposed that the mass m of contaminant eliminated was contained in the pore volume V_{pore}. The integral below the curves is therefore the same for all three curves:

$$m = \int_0^\infty c \cdot dV = c_0 \cdot V_{pore}$$

Curve d finally depicts an example where the washing resembles an extraction (→ Liquid–Solid Extraction) because the contaminant is not contained in the pores only, but also in the solid (liquid inclusions or soluble solid matter). The integral under curve d is therefore not related to the pore volume V_{pore} but to a higher total quantity of contaminant.

Theoretically such curves could be used to determine the residual mother liquor content in the cake from analyses of the filtrate. In practice this is impossible since the required residual contents in the cake are much smaller than the precision of such a mass balance. Nevertheless analyses of the filtrate are often used to judge the progress of washing. This is possible if an empirical correlation between the two concentrations in the filtrate and in the cake exists for the

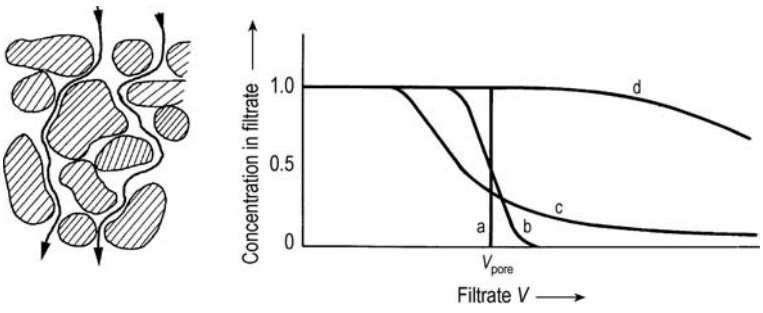

Figure 14. Concentration of contaminant in the effluent of a filter cake during washing a) Idealized piston flow; b) Effect of axial dispersion; c) Effect of diffusion from dead-end pores; d) Effect of contaminant extracted from the solid

particular process. The validity of such empirical correlation is, however, restricted to the particular equipment and operating parameters.

3.2. Example of Experimental Results

An illustrative example of a washing process is given in Figure 15 A and B [22]. A kaolinite suspension contaminated with NaCl was filtered to varying cake thickness and washed with varying quantities of water. After every test the residual salt content in the cake was measured and the results are reported as a function of washing time and of wash ratio. (In contrast to Fig. 14 the wash-ratio is related to the solids mass, not the pore volume. Also the residual content of the cake is reported, not the concentration in the filtrate)

Figure 15 A shows how at the very beginning of the washing process the residual concentration depends on the wash ratio, disregarding the cake thickness. In this example this is true up to the dash-dotted line which corresponds to less than a one-fold displacement of the pore volume. As the wash ratio increases to several times the pore volume, the mechanism of axial dispersion becomes more important, and the effect of a given quantity of wash liquid becomes better for thick cakes than for thin ones.

Figure 15 B shows how at the end of an experiment the washing time is the most relevant parameter for the result. In this example this seems to be true below a residual concentration of

$$\frac{c}{c_0} \approx 10^{-3}$$

3.3. Test Procedures and Pitfalls

As can be seen in Figure 15, washing of filter cakes gives scattering results even under laboratory conditions. This explains why only few experimental results are found in the literature: many experimentators are discouraged by inconclusive test results and never publish them. The reason of scattering results are stochastic influences:

Fingering. In most washing processes the wash liquid has a lower viscosity than the mother liquor. It tends to flow through the cake in finger-like streams past isles of viscous fluid, as shown in Figure 16 [22]. This is a stochastic process,

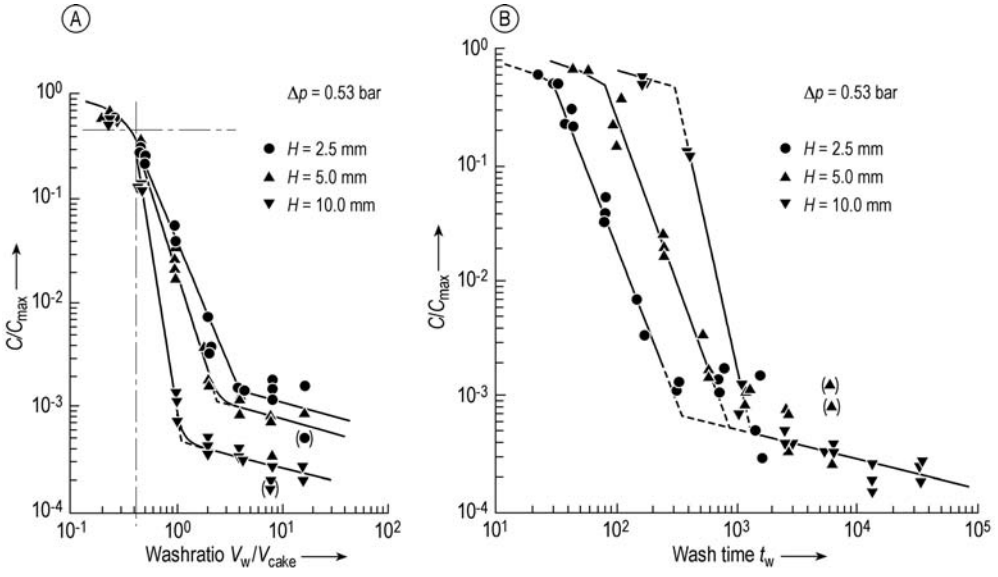

Figure 15. Residual concentration of salt in filter cakes of kaolin A) Test results reported as a function of the quantity of wash water; B) Test results reported as a function of washing time [22]

and the local concentration in the cake and the momentary concentration in the effluent will vary stochastically. Scale-up from a laboratory test filter with only small-scale fingering can be misleading as well as the results of few small samples taken from a big cake.

Instabilities Shrinking. If small electrodes are placed in a filter cake during the washing process, they indicate wildly varying local conductivity. This reveals the existence of small cracks in changing size and positions even in cakes with no visible fissures or shrinkage. This is not surprising because the contact forces between the particles change dramatically when the ion content of the surrounding liquid is washed off (see Chap. 6). The phenomenon has not yet been investigated thoroughly, but its stochastic effects on the washing results should be similar to the above-mentioned fingering.

If shrinking during washing presents a serious problem, it can be helpful to reslurry the cake in wash liquid and filter it again. Many nutsche filters (→ Filtration, 2. Equipment, Chap. 3.) are used this way. The second cake (with less ions in the liquid during cake build-up) is often less porous and less prone to shrinking (but also less permeable) than the original one.

In order to get meaningful results from washing experiments in spite of all these pitfalls, the following procedure is useful (see Fig. 17). Wash liquid flows at constant pressure through the cake. The quantity of filtrate and its composition are recorded automatically. Often the pH and the conductivity Q of the filtrate are used as indicators for concentration; sometimes its color may be more informative. The washing is continued until the filtrate reaches a pre-set criterion for purity (chosen according to some preliminary experience so that cake purity is near to the required specification). At this point the flow of wash water is automatically stopped. This should be done automatically, since it will probably happen during the night. The next morning, the cake is deliquored by air blowing and its residual content is analyzed. In small-scale experiments the whole cake should be analyzed, in large-scale experiments several samples must be taken from different parts of the cake.

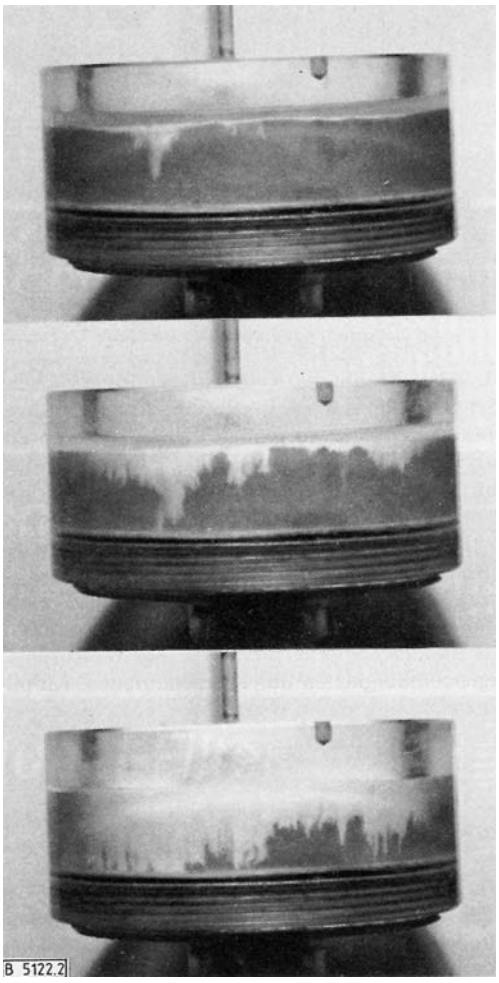

Figure 16. Visualization of *fingering* flow in a transparent laboratory nutsche filter. A wash liquid of lower viscosity displaces dark mother liquor [22]

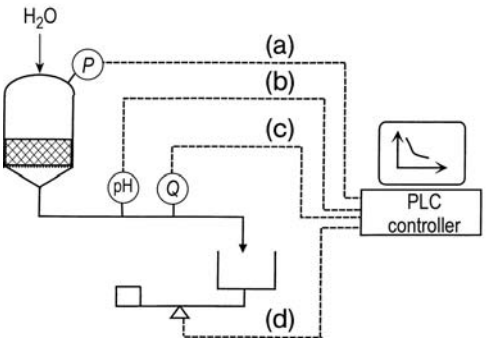

Figure 17. Test arrangement for washing test a) Pressure; b) pH; c) Conductivity; d) Weight

The following results must then be evaluated:

1. The required washing time
2. The required quantity of wash liquid
3. The resulting purity of the cake

Each of these criteria will scatter stochastically, but considering all three together a meaningful interpretation will result.

3.4. "Intermediate" Deliquoring before Cake Washing

Normally it is advantageous to deliquor the cake partly before washing, thus reducing the amount of mother liquor to be washed out. Sometimes, however, this "intermediate" deliquoring has detrimental effects:

If deliquoring is done by gas pressure, cracks may appear which let pass the washing liquid (see Section 4.1). In this case any deliquoring before the washing has to be avoided carefully. On belt filters (→ Filtration, 2. Equipment, Chap. 10.) an overlap of filtering and washing zones is therefore often accepted, even if mother liquid and wash liquid get mixed. Some nutsche filters (→ Filtration, 2. Equipment, Chap. 3.) have even been equipped with optical sensors to avoid premature deliquoring [23]. They measure the light reflected by the liquid surface and detect when the cake surface runs dry, so that the gas pressure can be released before cracks appear.

If deliquoring is done by compression (see Section 4.2), the cake may get rather impermeable. Thus, according to a rule-of-thumb the applied pressure should be raised monotonously during the sequence of filtering–intermediate deliquoring–washing–final deliquoring, i.e., the squeezing pressure for intermediate deliquoring should be lower than the pressure for washing.

4. Deliquoring of Filter Cakes

4.1. Deliquoring by Gas Pressure

The moisture in the pores of a filter cake can be displaced by gas flowing through the cake under pressure. The residual saturation with moisture as a function of time then asymptotically approaches a final equilibrium value as represented in Figure 18. Thus, an equilibrium is established with regard to mechanical displacement of the liquid. Thermal drying by airflow will of course further reduce the moisture down to total dryness if the air flows long enough. But generally thermal effects are small as compared with mechanical effects because of the comparably small mass of air flowing through a filter cake [24].

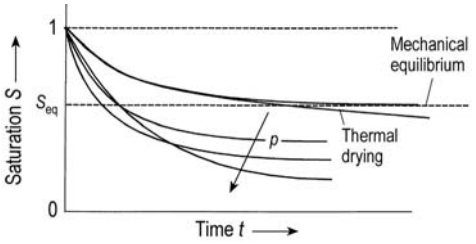

Figure 18. Deliquoring by gas pressure — residual saturation as a function of time

The final *equilibrium* moisture for mechanical dewatering depends on the nature of the cake and the applied pressure difference. The initial deliquoring speed however depends in addition on the cake thickness. For both values the flow rate of gas is apparently without importance, if it is not to produce the pressure difference. In the next sections first the equilibrium conditions will be examined.

4.1.1. Equilibrium Saturation of Filter Cakes

A plot of saturation of the cake versus pressure difference in an equilibrium state is called a *capillary pressure curve*. It can be measured in a device according to Figure 19 [25]. The saturated filter cake (b) is placed in the filter (a) on a filter media (c) (e.g., semipermeable microporous membrane, the membrane is permeable for liquid, but it is impermeable for gas at the applied pressure). Gas pressure is applied via port (e). The quantity of liquid displaced from the cake is drained by the valve (d) and collected. The standpipe is used to obtain an exact liquid level when the pressure gauge is adjusted to zero.

A typical capillary pressure curve is shown in Figure 20 (material: incompressible cake of glass beads with a mean diameter of 79 μm and

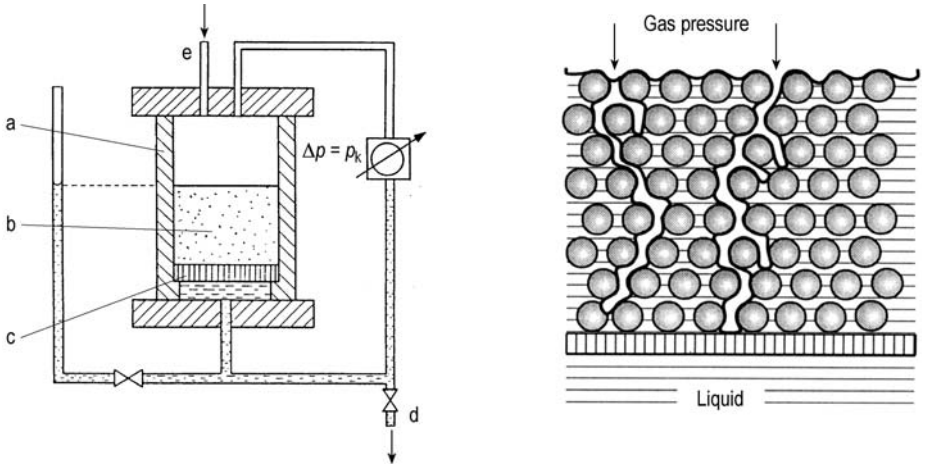

Figure 19. Test installation for measuring the capillary pressure p_k [25] a) Filter vessel; b) Filter cake; c) Semipermeable membrane; d) Draine; e) Entry for gas

water). Starting from the completely saturated cake ($S = 1$) the gas pressure is slowly increased, at each set point the equilibrium is established and the quantity of displaced liquid is registered, yielding a point of the deliquoring curve. Liquid is displaced from the pores when the pressure exceeds a certain threshold pressure. This is the capillary entry pressure p_{ce} (in this example 0.062 bar). Each time when a pore is emptied, the gas pressure overcomes the capillary pressure at the neck of the pores with a diameter $d_{pore,neck}$:

$$p_{ce} = \frac{4 \cdot \sigma \cdot \cos\delta}{d_{pore,neck}} \tag{23}$$

Further increase of the pressure displaces liquid from finer pores and reduces the moisture down to an irreducible saturation S_∞ after infinite time beyond which no further reduction is reached. This corresponds to the amount of liquid, which is trapped in isolated domains within the cake.

Figure 20 also shows the *imbibition curve*. When the pressure is reduced again, and provided that the bottom of the cake is still in contact with the expelled liquid, then the cake will be reimbibed by capillary suction. At equal moisture content the suction pressure will be smaller than the capillary pressure difference for deliquoring. This is easily explained because the capillary pressure for imbibition depends on the larger *waist*-diameter of the pores (see Fig. 20):

$$p_{ci} = \frac{4 \cdot \sigma \cdot \cos\delta}{d_{pore,waist}}$$

Also imbibition does not go to full saturation, because some air remains trapped in the pores.

The following conclusions can be drawn from the capillary pressure curve:

1. Deliquoring is caused by pressure difference between gas and liquid. Gas flow is normally required to maintain this pressure difference,

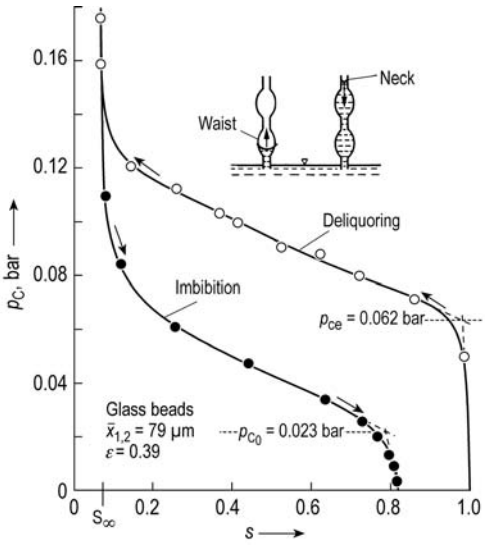

Figure 20. Example of a capillary pressure curve for imbibition and for deliquoring [25]

but not for the deliquoring itself. No gas flow is necessary if the cake is placed on a semipermeable membrane, which is impermeable for gas. (This principle can also be used technically for dewatering without gas flow [26])

2. A certain threshold pressure must be exceeded before liquid is displaced from the pores; this is the capillary entry pressure p_{ce}. This implies technical consequences:
3. Vacuum filters are restricted to pressure differences < 1 bar. This means that cakes cannot be deliquored by suction if their p_{ce} is near or above this limit. A pressure filter with $\Delta p > 1$ bar has to be considered for such cakes, even if its installation is much more expensive than that of a vacuum filter. Theoretically suction can dewater filter cakes with pores $>$ ca. 3 μm: with pure water and a small contact angle ($\delta \approx 0$) Equation (23) yields $p = 1$ bar for $d_{pore} = 2{,}9$ μm.

Filter cakes of submicronic particles like wastewater sludge have such a high capillary entry pressure that their pores cannot be dewatered mechanically: with pure water and a small contact angle Equation (23) yields $p > 10$ bar for $d_{pore} < 0.29$ μm.

4.1.2. Kinetics of Deliquoring by Gas Pressure

In most cases there is no semipermeable membrane below the cake but a *normal* filter medium that is permeable for gas, like a filter cloth. Gas and liquid flow simultaneously through the cake. The gas exerts capillary pressure onto the adjacent liquid and both gas and liquid flow in the same direction, however, with different speeds and different pressures (the local pressure difference between gas and liquid is equal to the local capillary pressure). The difference in saturation between bottom and top of an incompressible filter cake is normally rather small, see Figure 21 A. This is in contrast to the deliquoring by gravity (or by a centrifugal field), shown in Figure 21 B. In this latter case always a saturated bottom layer exists, corresponding to the capillary suction height of the cake. Even in equilibrium this layer remains saturated. Sometimes this height is negligibly small. In scraper-type centrifuges (→ Centrifuges, Filtering) for example, the saturated bottom layer must be smaller than the residual layer which the scraper does not remove.

The permeability of a completely saturated cake is the same if either liquid or gas flows through the pores. When, however, gas and liquid flow simultaneously through the cake, the pores filled with liquid and the pores filled with gas form two separate capillary systems, each of them with reduced permeability. The local permeabilities (for liquid or air) in relation to the permeability of the saturated cake are called *relative permeabilities* k_{rel}. They depend on the local saturation of the cake and can be represented as:

for the wetting fluid (the liquid)

$$k_{rel,w} = \frac{k_w}{k} = \frac{\alpha}{\alpha_w}$$

for the nonwetting fluid (the gas)

$$k_{rel,n} = \frac{k_n}{k} = \frac{\alpha}{\alpha_n}$$

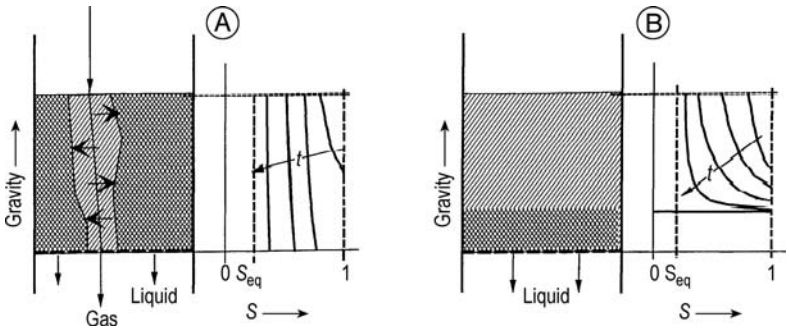

Figure 21. Kinetics of deliquoring A) Deliquoring by gas blowing; B) Deliquoring by gravity or a centrifugal field

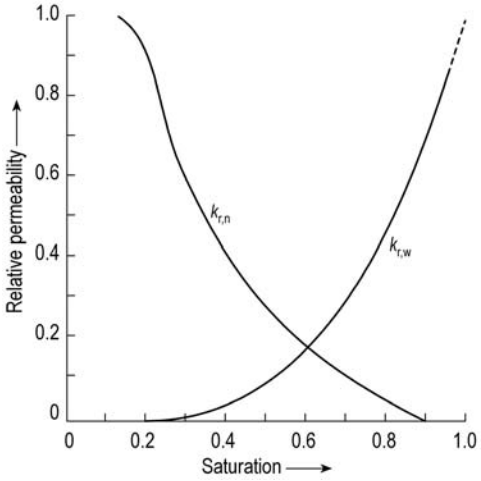

Figure 22. Relative permeability as a function of saturation [27]

Such relative permeabilities are shown schematically in Figure 22 as a function of cake saturation [27]. The permeability for the liquid (the wetting phase) declines to zero at a finite saturation. This value corresponds to the irreducible saturation S_∞. At the other extreme the flow of air ceases when the saturation is above 90 %. Some of the voids are filled with air without allowing an appreciable airflow.

If the curves for capillary pressure and for the relative permeabilities as a function of saturation are known, the local values of capillary pressure, gas permeability, and liquid permeability are defined as functions of the local saturation. The deliquoring kinetics by gas flow can then be described mathematically. The resulting system of interdependent differential equations is however extremely complex and not suited for practical application. For scientific purposes approximate solutions have been verified by comparing them to experiments [25].

4.1.3. Approximate Solution for Coarse, Incompressible Cakes

For the particular case of incompressible cakes with threshold pressures much smaller than the applied gas pressure $p_{ce} \ll p$ (hence for rather coarse solid particles), WAKEMAN has described the process of deliquoring by gas pressure by three dimensionless parameters [28]:

reduced saturation

$$S_R = \frac{S}{1-S_\infty}$$

dimensionless time

$$\Theta = \frac{p_{ce} \cdot t}{\alpha_H \cdot \eta \cdot H^2 \cdot (1-S_\infty) \cdot \varepsilon}$$

dimensionless pressure difference

$$\Delta P = \frac{p_{entry}}{p_{ce}} - \frac{p_{exit}}{p_{ce}}$$

According to this approach, the cake is characterized by its porosity e, the filter resistance α_H (of the saturated cake) and the capillary pressure curve which itself is approximately described by the capillary entry pressure p_{ce} and the "irreducible" saturation S_∞ (see Fig. 20). The relative permeabilities are described by generalized interpolation formula. With these approximations the residual saturation and the theoretical gas flow rate can be read from the dimensionless charts, shown in Figures 23 and 24. An example how to apply these charts is given in [29]. However, the validity of these charts is limited to $p_{ce} \ll p$ and to incompressible cakes. Also the gas flow rate indicated on the chart does not take into account the possibility of cracks in the cake which can increase the gas flow tremendously (see Section 4.1.5).

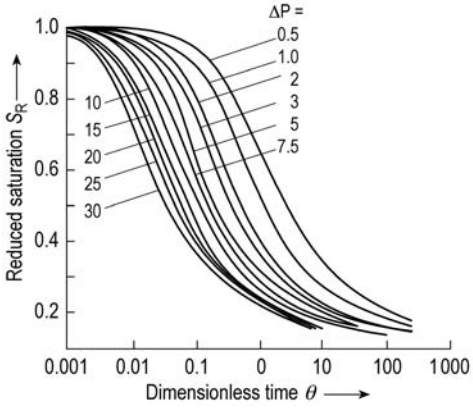

Figure 23. Reduced cake saturation vs. dimensionless time [29]

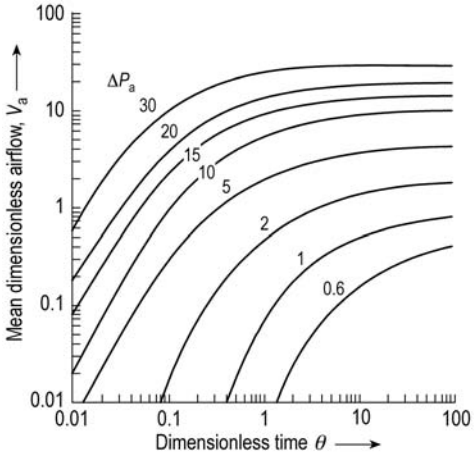

Figure 24. Reduced air (gas) flow rate vs. dimensionless time (WAKEMAN and PURCHAS 1986; reproduced from [29])

4.1.4. Practical Scale-Up of Deliquoring by Gas Pressure

The deliquoring kinetics are normally investigated by measuring the residual moisture as a function of cake thickness, blowing time, and pressure difference. The results are interpolated to give the parameters necessary for scale-up. Extrapolation beyond the investigated range of cake thickness, blowing time, and pressure should be avoided. In addition it is important to measure and to scale-up the gas flow from realistic experiments, since in most cases the capacity of the compressor is the limiting factor, not the pressure. Particular attention has to be paid to the possible formation of cracks. In case of doubt, a filter test with sufficiently large filter area is recommended, because the cracks may not be pronounced and obvious on a small laboratory filter. Typically the cracks appear at a characteristic liquid saturation which then represents the limit for deliquoring by gas blowing with technically reasonable gas flow rates (see Section 4.1.5).

Interpolation of the test results with a minimum number of tests is easier if the residual moisture is reported as a function of a dimensionless time Θ. The results from a given kind of filter cake are then supposed to fit approximately a straight line in a logarithmic chart. As a first approach, when nothing is known about the deliquoring behavior of the cake, the experimental values are reported as a function of

$$\Theta_0 = \frac{\Delta p \cdot t}{\eta \cdot H \cdot (\alpha \cdot H + \beta)} \approx \text{const} \cdot \frac{\Delta p \cdot t}{H^2}$$

Here $\Delta p = p_{\text{entry}} - p_{\text{exit}}$ is the pressure difference applied. This approach gives generally good results for centrifugal dewatering, as shown in Figure 25 (the pressure difference being calculated from the centrifugal force) [30]. For dewatering by gas blowing, the fit is, however, often unsatisfactory (see Fig. 26) [30]. A dimensionless time taking into account the capillary entry pressure p_{ce} will always permit a good fit. Two equations are proposed in the literature [30]:

$$\Theta_1 \approx \frac{\Delta p \cdot t}{\eta \cdot H \cdot (\alpha \cdot H + \beta)} \cdot \frac{p_{\text{entry}}}{p_{\text{exit}}} \cdot \left(1 - \frac{p_{\text{ce}}}{\Delta p}\right)$$

$$\approx \text{const} \cdot \frac{\Delta p \cdot t}{H^2} \cdot \frac{p_{\text{entry}}}{p_{\text{exit}}} \cdot \left(1 - \frac{p_{\text{ce}}}{\Delta p}\right)$$

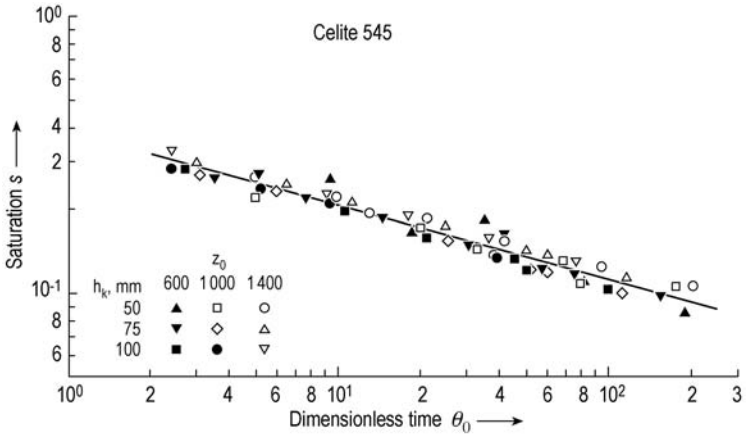

Figure 25. Residual saturation of filter cakes dewatered by centrifugal force as a function of dimensionless time Θ_0 [30]

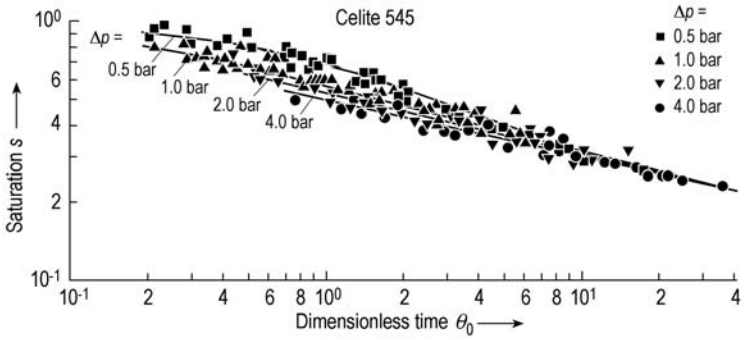

Figure 26. Residual saturation of filter cakes dewatered by gas blowing as a function of dimensionless time Θ_0 [30]

and [31]

$$\Theta_1 \approx \frac{\Delta p \cdot t}{\alpha \cdot \eta \cdot H^2} \cdot \frac{2}{\varepsilon} \cdot \left(1 - \frac{p_{ce}}{\Delta p}\right)$$

$$\approx \text{const} \cdot \frac{\Delta p \cdot t}{H^2} \left(1 - \frac{p_{ce}}{\Delta p}\right)$$

Here p_{entry} and p_{exit} are the pressures applied above and below the cake and p_{ce} is the capillary entry pressure. This p_{ce} is not measured, but derived as a "best fit" to the experiments (this is why the fit is generally rather good, see Figure 27 [30]).

4.1.5. Shrinking and Cracks in Filter Cakes

Deliquoring of compressible filter cakes by gas pressure very often produces cracks in the cake, a problem of great practical impact. The mechanism of crack formation is represented in Figure 28. During filtration the viscous forces from the flowing liquid compress the cake. As described in Section 2.2, only the layer near the filter medium is subjected to the full amount of pressure, while the "upper" layer of the cake remains uncompressed (Fig. 29 (1)). When filtration is finished, the liquid surface reaches the cake surface (Fig. 29 (2)). Before gas enters into the capillaries of the cake, the capillary entry pressure p_{ce} must be overcome. The surface tension of the liquid thus exerts a pressure $p \leq p_{ce}$ onto the cake, comparable to an elastic membrane spread over the cake. As long as p_{ce} is not exceeded, the cake is compressed monoaxially like by action of a piston, the cake thickness is reduced, but no cracks appear. However, when p_{ce} is exceeded, gas penetrates into the largest capillaries, and the solid structure is com-

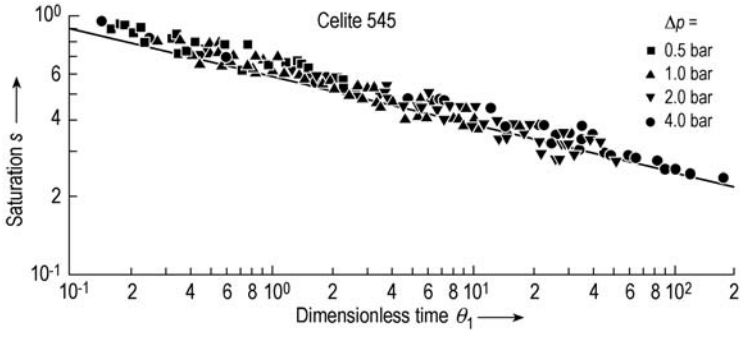

Figure 27. Residual saturation of filter cakes dewatered by centrifugal force as a function of the modified dimensionless time Θ_1 [30]

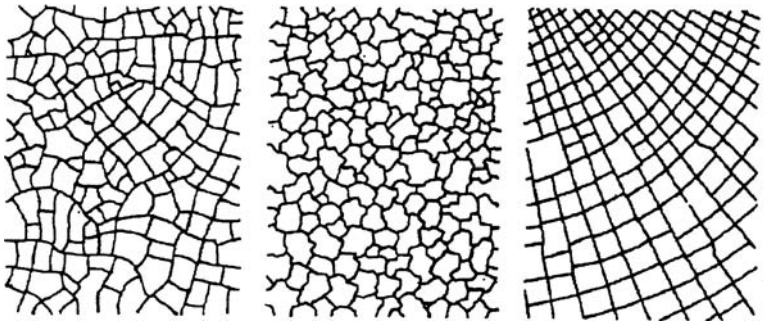

Figure 28. Formation of cracks by gas blowing through a compressible cake

pressed by lateral forces. This and the capillary forces may lead to lateral compression of the cake and hence to cracks (Fig. 29 (3-4)). The criterion for cracks to occur thus probably depends on the lateral compressive strength of a cake after monoaxial consolidation. But until now the precise mechanism of crack formation is not understood and the great variety of crack patterns shown in Figure 28 [32] cannot be explained.

Cracks in a filter cake are very detrimental to further deliquoring and also to subsequent washing (see Chap. 3) because gas and wash liquid flow through the cracks without great resistance and without effect. The only sure remedy against cracks is compression of the cake before gas blowing. When the remaining *shrinking potential* (this is the remaining shrink when the cake is reduced to total dryness) is small enough, no cracks will appear anymore [33]. Some filters are equipped for this purpose with membranes or with pressure belts (→ Filtration, 2. Equipment, Section 7.3.). According to a proposal of SHIRATO and coworkers this compression can also be achieved by adding a layer of very fine material (hence a cake layer with high p_{ce}) onto the surface of the cake [34].

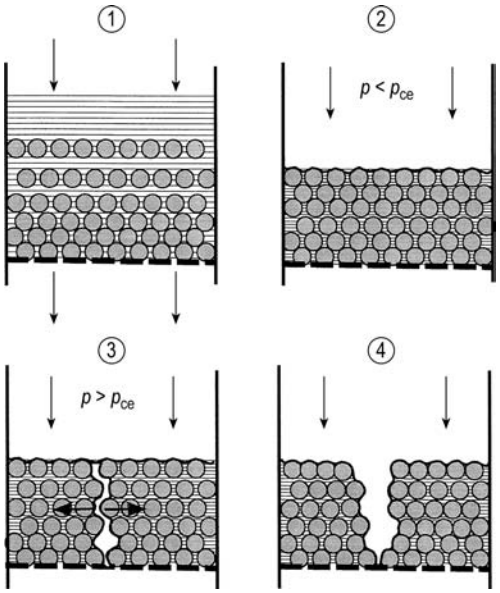

Figure 29. Patterns of shrinking cracks [32]

Some remedy against cracks is also possible with nutsches equipped with agitators (→ Filtration, 2. Equipment, Chap. 3.). With their paddles they smear over the surface of the cake during deliquoring so that the cracks are closed as soon as they appear. This does, however, not eliminate the cracks totally but only down to a certain depth below the surface of the cake, so that some cracks can exist invisibly below the surface. Without such equipment the formation of cracks can be reduced (but only to a very limited degree) if the cake is formed with high final filtration pressure, and hence with somewhat less porosity.

4.2. Deliquoring by Expression

When soft filter cakes are compressed, the void volume of the cake is reduced by expelling liquid, while the voids remain saturated with liquid. Such compression often is applied in combination with a subsequent deliquoring by

gas pressure; it reduces the subsequent gas flow and prevents the formation of cracks (see Section 4.1.5). But there are many applications where deliquoring by gas pressure is not possible, and expression is the only way to reduce the liquid content by mechanical means. Classical examples for applications of mechanical forces are juice and oil pressing from fruits and also the dewatering of wastewater sludge in membrane filter presses or in pressure belt filters (→ Filtration, 2. Equipment, Chap. 8.). Such sludges form filter cakes with very high capillary entry pressure p_{ce} so that deliquoring by gas blowing is technically not feasible.

Mathematical description of expression generally starts from modifications of the Terzaghi model for soil mechanics. The ratio of liquid collected to the amount of liquid, which can be expressed, is [35]

$$U_c = \frac{H_1 - H(t)}{H_1 - H_\infty} = 1 - B \cdot \exp(-C \cdot t)$$

where U_c is the consolidation rate, $H(t)$ the cake thickness, H_1 the original cake thickness and H_∞ the thickness after infinite time. B and C are *creep* constants and t_c is the consolidation (= compression) time. A comparison of different compression models can be found in [36].

5. Optimal Filtration Cycle Time

When sizing a filter installation, the right filtration cycle time has to be chosen (example: the same task can be performed in a small filter which must be cleaned frequently or a bigger one with longer cycles). With a long filtration time the filter cake becomes thick and the flow rate per filter area declines. On the other hand for very short filtration the downtime for frequent cleaning will reduce the capacity. This leads to two questions: (1) What is the optimal cycle time with the highest overall throughput? (2) What is the optimal cycle time with the lowest overall cost?

1. Figure 30 shows the quantity of filtrate produced as a function of time. Before the start of filtration a time t_{reg} is needed for regenerating the filter (extracting the cake from the previous cycle, cleaning the filter, rearranging the filter elements, etc.). The highest overall throughput is obtained when the straight line from the start of this regeneration to the end of filtration is tangential to the yield curve. In other words: the filtration should be stopped when the instantaneous flow (as indicated by a flow meter) falls below the mean throughput according to the definition:

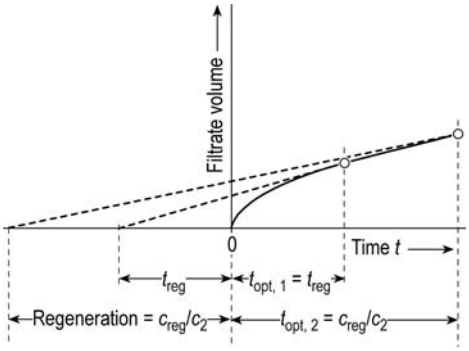

Figure 30. Optimal cycle time derived from the yield curve; $t_{opt,1}$ for maximal flow per time and $t_{opt,2}$ for maximal yield per cost

$$\dot{V}_{mean} = \frac{V}{t + t_{reg}} \tag{24}$$

This criterion can for example be implemented in a computerized process control. For design purposes it can be useful to calculate the optimal cycle time in advance. For this purpose a rule-of-thumb will be derived assuming cake filtration and negligible resistance of the filter medium ($\beta = 0$). The quantity of filtrate according to Equation (10) or (11) is then

$$V = c_1 \cdot t^{1/2} \tag{25}$$

and Equation (24) becomes

$$\dot{V}_{mean} = \frac{c_1 \cdot t^{1/2}}{t + t_{reg}}$$

The highest $\dot{V}_{mean}$ is obtained if the filtration is stopped at t_{opt}, which is defined by the differential equation

$$\frac{d}{dt}\left(\frac{1}{\dot{V}_{mean}}\right) = 0 = \frac{1}{2c_1} \cdot t_{opt}^{-1/2} - \frac{t_{reg}}{2c_1} \cdot t_{opt}^{-3/2}$$

This leads to the rule-of-thumb for maximum throughput:

$$t_{opt,1} = t_{reg}$$

This rule is valid if the influence of the filter medium resitance is neglected ($\beta = 0$).

2. Quite analogous considerations are valid for the optimal cycle time in terms of cost per quantity filtered. During filtration, the running cost is proportional to time (capital cost and pumping energy), cost $= c_2 t$. In Figure 30 all costs are converted with this proportionality factor c_2 into an equivalent running time: $t = \text{cost}/c_2$.Regeneration represents a considerable cost, including downtime, labor, new filter elements, and disposal of waste. If this cost is called c_{reg}, the mean specific cost is

$$\frac{\text{cost}}{\text{filtrate}} = \frac{c_2 \cdot t + c_{reg}}{V}$$

With the approximation of Equation (25) this is

$$\frac{\text{cost}}{\text{filtrate}} = \frac{c_2}{c_1} \cdot t_{opt,2}^{1/2} + \frac{c_{reg}}{c_1} \cdot t_{opt,2}^{-1/2}$$

The minimum is defined by

$$\frac{d}{dt}\left(\frac{\text{cost}}{\text{filtrate}}\right) = 0 = \frac{c_2}{2c_1} \cdot t_{opt,2}^{-1/2} - \frac{c_{reg}}{2c_1} \cdot t_{opt,2}^{-3/2}$$

As result the rule-of-thumb for maximal yield per cost is obtained:

$$c_2 \cdot t_{opt,2} = c_{reg}$$

or *cost for the filter run = cost for regenerating the filter*.

These rules have been derived here for constant pressure filtration. They can also be derived for filter runs with different but constant flow rates until a pre-set final pressure. Practitioners therefore apply the rule-of-thumb rather generally (e.g., also for filtration with a pump with a characteristic curve anywhere between constant pressure and constant flow).

6. Interparticle Forces and Forces Between Particles and Filtermedia, DLVO Theory

According to the theory of Derjaguin, Landau, Verwey, and Overbeek (DLVO theory), the forces between suspended particles of equal material are described by repulsion due to electrostatic charges and attraction due to van der Waals' forces:

Repulsion. Particles in suspension (especially in polar liquids like water) have an electrically charged surface due to adsorption and dissolution of ions. The order of magnitude of this charge ζ is $-120\ \text{mV} < \zeta < 120\ \text{mV}$, and it depends on the pH of the liquid. The charge reaches relatively far, depending on the ion content of the surrounding liquid. The reach is characterized by the Debye length r_D. In pure distilled water this length is exceptionally long with 0.9 μm. In most technical aqueous solutions it is much smaller, in sea water for example only 0.4 nm [37].

Attraction. Van der Waals forces are part of the cohesive forces between the molecules within the solid particle. They reach also a certain distance beyond the surface, but their range is less than that of electrostatic forces. The decline is proportional to the distance according to

$$E_{attraction} = -\frac{\text{const}}{r}$$

When two particles approach to distance zero, these attractive forces become very strong and should in principle become equal to the cohesive force inside the particle. The reality is, however, more complicated because there are always absorbed molecules on the surface.

An example of the superposition of both forces according to DLVO theory is represented in Figure 31. The graph shows the resulting energy potential. A positive gradient of the curves describes attraction, negative gradient repulsion. At very small distances, attraction prevails. At larger distance electrostatic repulsion prevails (if it is not zero).

Attraction and repulsion between two particles in suspension. The superposition of electrostatic repulsion and attraction by van der Waals forces is represented by the resulting energy potential. High ion content in the surrounding liquid reduces the reach of electrostatic repulsion (Debye length)

Interparticle contact. Electrostatically charged particles repulse one another. In com-

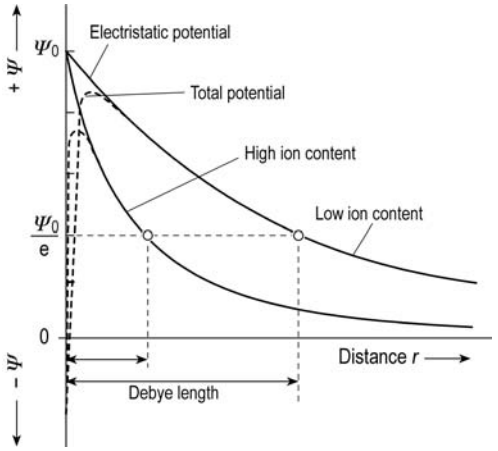

Figure 31. Energy potential vs. particle distance (DLVO-theory)

parison to their equally charged neighbors they show some kind of smooth and slippery repulsive skin. (The smooth repulsive skin can be made visible with modern atomic force microscopy, see [38].) The Debye length characterizes the thickness of this skin (see Fig. 32).

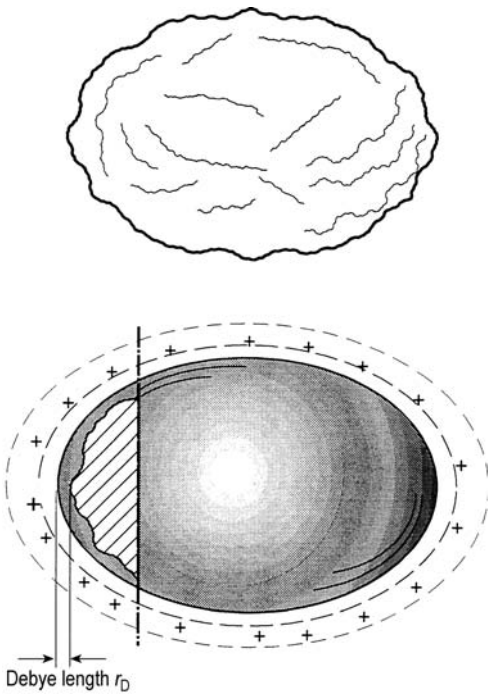

Figure 32. A particle in suspension

Without electric charge, there is no such skin. The particles touch their neighbors with their rough surfaces and tend to adhere due to van der Waals' forces.

Particles in aqueous suspension with weak electric charge most probably have oppositely charged patches on their surface what may enhance mutual adhesion and the formation of loose flocs.

In comparison to particles with the same surface charge, it is covered with a repulsive skin of a thickness near the Debye length. This skin has no roughness and no friction; hence it is rather slippery

The surface charge of suspended particles can be measured as a *zeta potential* (→ Colloids, Chap. 4.; → Emulsions, Section 11.6.). This potential varies with the suspending liquid, especially with its pH: High pH means a high concentration of OH^- ions, which can be absorbed, creating a negative surface charge. Low pH means high concentration of protons and a positive surface charge. At a certain pH the surface is neutral (point of zero charge, isoelectric point). At this particular pH, the particles can more easily agglomerate and are easier to filter. This optimal pH is often determined empirically without knowledge of the zeta potential.

7. Mathematical Simulation of Filtration and Cake Formation

Different attempts have been made to simulate numerically the structure and porosity of filter cakes. Until now such calculations are restricted to spherical particles with homogeneous surface. Starting from randomly chosen locations the trajectories of particles in a filter flow are calculated. When they touch the cake surface, the deposition is simulated using either a sticking angle [39, 40], or a friction angle and an adhesive force [41, 42], or by estimating the interparticle forces from van der Waals' and electrostatic forces according to the DLVO theory [43]. After calculating the deposition of a large number of particles, the packing density of the resulting cake is found (see Figure 33 A and B). These calcula-

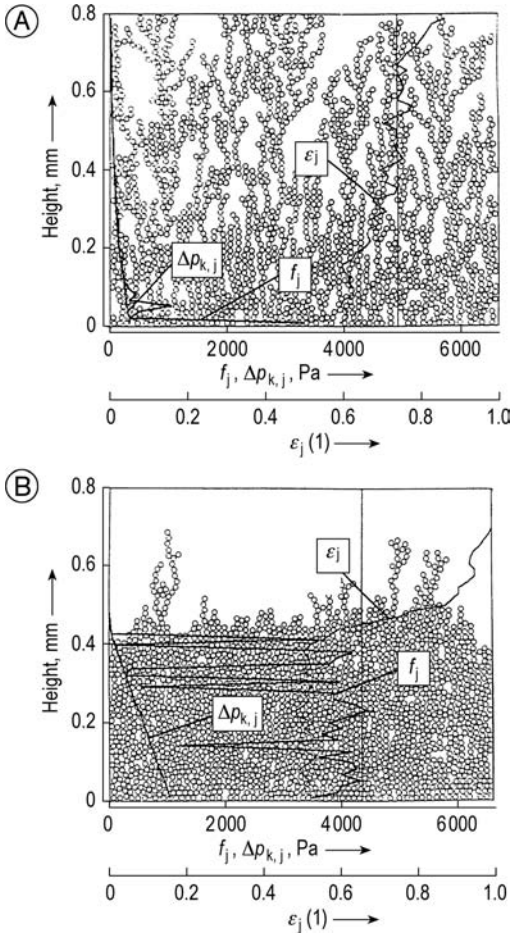

Figure 33. Simulation of the cake build-up for two different adhesion forces and friction angles A) For 4×10^{-8} N adhesion force and 20° friction angle; B) For 1×10^{-8} N adhesion force and 5° friction angle [42]

tions help to understand and explain some empirical facts:

1. High adhesion forces and large friction angles make the particles adhere at the first contact and produce a randomly stacked *house of cards* with high porosity and permeability. Low adhesion forces or even repulsion between the particles make them slip to more stable positions and produce dense packing. Figure 33 A and B shows the cake structure calculated by a two dimensional simulation for different friction angles and adhesive forces [42].
2. An opposite effect can be observed when the particles are very small (colloidal). Here the Debye length is often not negligible compared to the particle size and the repulsion can be strong enough to keep the particles at a distance. In this case the porosity and permeability will increase by repulsion and decrease by adhesion, contrary to what was said above. This is for example observed with clay soil in marshland near the sea. The permeability of such soil is reduced after flooding with salt water and increases again when the salt is washed out, i.e., the Debeye length increases with falling ion content. For industrially filterable suspensions however the effect is not yet reported in the literature. It seems that for particles > 0.1 μm either the Debye length is to small (at high ion content) or the zeta potential is not strong enough (as in distilled water) for this effect.

A comprehensive simulation of cake formation has not yet been proposed. The above mentioned approaches are restricted to spherical particles with uniform surface charge. Often, however, the electric charge is unevenly distributed, and there may even exist oppositely charged spots on the same particle. This would explain why many suspensions form loose flocs when the stirrer is stopped. This is quite often observed even if the pH is not exactly at the isoelectric point (the term *isoelectric range* would therefore be more appropriate than *isoelectric point*). The flocs disappear when the stirrer starts again, but nevertheless they probably have an impact on filterability because the particles are prearranged in a way that they touch with their rough, adhesive spots and have less tendency to slip into densely packed positions when deposited on the filter cake.

8. Handling of "Unfilterable" Suspension

In industrial filtration often suspensions are encountered with a high filter resistance. Several possibilities for handling of these *unfilterable* suspensions are given below.

8.1. Optimization of Upstream Steps (Crystallization, Precipitation)

Considerable improvements in filterability are achieved by producing coarser particles. Good knowledge is available about crystallization (→ Crystallization and Precipitation). If, however, the solids are formed by precipitation, i.e., by mixing two reactants, this quick process often depends strongly on the mixing conditions and the reaction speeds. In this case the filterability must be improved empirically. Improvement has been achieved with the following parameters:

1. Continuous mixing instead of batch mixing
2. Recycling of suspended solids to the zone of solids formation
3. Variation of temperature, mixing ratio, stirring speed etc.

8.2. Application of Flocculants (Polyelectrolytes)

Synthetic, water-soluble polymers are highly effective as flocculating agents. They agglomerate fine particles in aqueous dispersion to voluminous flocs, which settle and filter easily. As a general rule, however, the resulting filter cake or sediment has a higher porosity and residual moisture than without flocculation.

Synthetic flocculants are commercially available as nonionic, anionic, or cationic grades with more or less ionic character. A charge opposite to the zeta potential of the solids to be separated gives theoretically the best effect. In practice it is, however, easier to observe the flocculation visually without knowledge of the surface charge. Samples of the suspension are prepared in graduated cylinders and gently mixed with different flocculants in 0.1 % solution. The high dilution is necessary to reduce the viscosity and facilitate mixing. The required quantity of polyelectrolyte is generally in the range of 0.5–10 kg per ton dry solids, equivalent to 10–100 mL of solution for 1 L suspension.

Criteria for the flocculation effect are settling speed, clarity of the supernatant, and aspects of the flocs (small, dense flocs are sometimes preferred, because they are more stable).

8.3. Adaptation of pH

As explained in Chapter 6, the interparticle forces depend on the pH of the surrounding liquid. With a pH in the isoelectric range the particles can aggregate and their filter resistance and settling speed is increased.

8.4. Checking of Alternatives to Cake Filtration

Possible alternatives to filtration are processing in:

1. Settling centrifuges (→ Centrifuges, Sedimenting) or static settlers. Even poorly filterable suspensions sometimes settle readily, either the solids have high specific weight or big, soft flocs make an impermeable cake (e.g., wastewater sludge)
2. Cross-flow filtration (see Section 2.5). This alternative, however, yields the solids as a thickened suspension only
3. Evaporation of the liquid (→ Evaporation). This alternative may be attractive if the required energy is not to high (highly concentrated suspension or a liquid with moderate heat of evaporation, like many organic solvents)

8.5. Use of a Filter Aid

Filter aids are inert powders added to the liquid to be filtered and increasing the porosity and permeability of the cake (→ Filtration, 2. Equipment, Chap. 16.). They are very helpful, provided the presence of filter aid in the solid can be accepted. Filter aids are used in two ways:

- As a precoat layer to protect the filter medium and improve filtrate clarity
- As a body feed to increase flow rates

Preliminary laboratory tests help to identify the proper kind of filter aid. The selection procedure is done in three steps:

1. Selection of the right material according to the chemical resistance and purity (perlite, diatomaceous earth, cellulose, carbon)
2. Selection of the grade (particle size) of the filter aid. The particle size should be as coarse as possible to give low filter resistance, but

fine enough to prevent the dirt particles from trickling through the pores of the cake. For selection of the grade a precoat layer is prepared by filtering a diluted suspension of filter aid. Then the solution to be cleaned is filtered through this layer. After filtration the precoat layer is broken in half. The dirt should form a separate layer on the top and should not have penetrated into the precoat

3. Selection of the quantity of filter aid. As a first guess the quantity of filter aid is calculated which gives a cake volume equal to the volume of dirt to be separated. It is then admixed to the suspension and the filterability of this mixture determined. If the flow rate is to low, the next trial should be made with a higher quantity of filter aid

References

1 H. Darcy: "Les fontaines publiques de la ville de Dijon," Paris 1856.
2 J. Kozeny, *Ber. Math.-naturwiss. Abt. Akad. Wien.* (1927) 271 – 306.
3 A. E. Scheidegger: *The Physics of Flow Through Porous Media*, 3rd ed., University of Toronto Press, Toronto 1974, pp. 137ff.
4 H. Rumpf, A. R. Gupte, *Chem. Ing. Tech.* **43** (1971) no. 6, 367 – 375.
5 W. Gösele, *Filtrieren Separieren* **9** (1995) no. 1, 14 – 22.
6 VDI-Richtlinie "Filtrierbarkeit von Suspensionen" VDI 2762, 1997.
7 "Filtrierbarkeit von Suspensionen, " *VDI-Richtlinie* **2762** (1997) .
8 J. Tichy: Fortschritt–Berichte VDI, Reihe 3, Nr. 877, Sonthofen (2007) .
9 L. Svarovsky: *Solid – Liquid Separation*, Butterworths, London 1977, p. 175.
10 M. Tiller, T. Cleveland, R. Lu, *Ind. Eng. Chem. Res.* **38** (1999) 590 – 595.
11 P. H. Hermans, H. L. Bredée, *Rec. Trav. Chim.* **54** (1935) 680 – 700.
12 A. Rushton, A. S. Ward, R. G. Holdich: *Solid – Liquid Filtration and Separation Technology*, VCH Verlagsgesellschaft, Weinheim, Germany, 1996, pp. 64 ff.
13 K. Luckert, *Wiss. Z. Techn. Univ. Magdeburg* **36** (1992) no. 5/6, 74 – 80.
14 P. L. Boucher, *J. Proc. Inst. Civ. Eng.* (1946 – 1947) 415 – 445.
15 A. Rushton, A. S. Ward, R. G. Holdich: *Solid – Liquid Filtration and Separation Technology*, VCH Verlagsgesellschaft, Weinheim, Germany, 1996, p. 198.
16 A. Rushton, A. S. Ward, R. G. Holdich: *Solid – Liquid Filtration and Separation Technology*, VCH Verlagsgesellschaft, Weinheim, Germany 1996, pp. 185 ff.
17 K. J. Ives, in A. Rushton (ed.): *Mathematical Models and Design Methods in Solid-Liquid Separation, NATO ASI series E No. 88*, Martinus Nijhoff, Dordrecht 1985, pp. 90 ff.
18 G. Dierckx in: *La Filtration Industrielle des Liquides, Tome III*, Société Belge de Filtration, Liège 1978, pp. 295 – 314.
19 A. Palinski, W. Uhl, R. Gimbel, *Vom Wasser* **89** (1997) 175 – 189.
20 J. Altmann, S. Ripperger, *J. Membrane Sci.* **124** (1997) 119 – 128.
21 S. Ripperger, J. Altmann, *Filtrieren Separieren* **11** (1997) no. 3, 109 – 113.
22 W. Bender, *Chem. Ing. Tech.* **55** (1983) no. 11, 823 – 829.
23 K.-H. Steiner, *Chem. Ing. Tech.* **61** (1989) no. 1, 1 – 8.
24 H. Anlauf, *Fortschrittsber. VDI, Reihe 3*, **114** (1986) .
25 H. Schubert: *Kapillarität in porösen Feststoffsystemen*, Springer Verlag, Heidelberg 1982, p. 184.
26 H. Anlauf, *Maschinenmarkt* **95** (1989) no. 8, 26 – 30.
27 R. J. Wakeman: "Cake Dewatering", in L. Svarovsky (ed.): *Solid – Liquid Separation*, Butterworths, London 1977, p. 300.
28 R. J. Wakeman, *Filtr. Sep.* **16** (1979) no. 6, 655 – 669.
29 A. Rushton, A. S. Ward, R. G. Holdich: *Solid – Liquid Filtration and Separation Technology*, VCH Verlagsgesellschaft, Weinheim, Germany, 1996, pp. 348 ff.
30 D. Redeker, K.-H. Steiner, U. Esser, *Chem. Ing. Tech.* **55** (1983) no. 11, 829 – 839.
31 I. Nicolaou, W. Stahl, *Aufbereit. Tech.* **33** (1992) no. 6, 328 – 338.
32 J. Walker, *Spektrum Wissensch.* **12** (1986) 188 – 197.
33 W. Tiedemann, *Fortschrittsber. VDI, Reihe 3*, **453** (1996) .
34 M. Shirato, T. Murase, E. Iritani, S. Nakatsuka, *Filtr. Sep.* **24** (1987) no. 2, 115 – 119.
35 A. Rushton, A. S. Ward, R. G. Holdich: *Solid – Liquid Filtration and Separation Technology*, VCH Verlagsgesellschaft, Weinheim, Germany 1996, pp. 455 ff.
36 D. Leclerc, S. Rebouillat, in A. Rushton (ed.): *Mathematical Models and Design Methods in Solid – Liquid Separation, NATO ASI series E No. 88*, Martinus Nijhoff, Dordrecht 1985, pp. 356 ff.
37 J. Gregory in K. J. Ives (ed.): *The Scientific Basis of Flocculation*, Sijdhoff & Noordhoff, Alphen aan de Rijn 1978, p. 91.
38 H.-J. Jacobasch, P. Weidenhammer, *Chem. Ing. Tech.* **68** (1996) 1590 – 1594.
39 D. Houi, R. Lenormand, in F. Family, D. P. Landau (eds.): *Kinetics of Aggregation and Gelation*, Elsevier, Amsterdam 1984.
40 P. Schmitz, B. Wandelt, D. Houi, M. Hildenbrand, *J. Membrane. Sci.* **84** (1993) 171 – 183.
41 W. Höflinger, C. Stöckelmayer, A. Hackl, *Filtr. Sep.* (1994) Dec., 807 – 811.
42 W. Höflinger, C. Stöckelmayer, *Staub Reinhalt. Luft* **55** (1995) 423 – 428.
43 W.-M. Lu, C. C. Lai, K.-J. Hwang, *Sep. Technol.* **5** (1995) 45 – 53.

Further Reading

G. G. Chase, E. Mayer: *Filtration*, "Kirk Othmer Encyclopedia of Chemical Technology", 5th ed., vol. 11, p. 321–397, John Wiley & Sons, Hoboken, 2005, online: DOI: 10.1002/0471238961.0609122019220118.a01.pub2 (March 2003)

K. Sutherland: *A-Z of Filtration and Related Separations*, 1st ed., Elsevier, Oxford 2005.

K. Sutherland: *Filters and Filtration Handbook*, 5th ed., Elsevier Butterworth-Heinemann, Amsterdam 2008.

R. J. Wakeman, E. S. Tarleton: *Solid/liquid Separation*, 1st ed., Elsevier, Oxford 2005.